



TAMPEREEN TEKNILLINEN YLIOPISTO
TAMPERE UNIVERSITY OF TECHNOLOGY

MUHAMMAD WAQAS AHMAD KHAN
STATISTICAL SENSOR FUSION OF ULTRA WIDE BAND RANGING
AND REAL TIME KINEMATIC SATELLITE NAVIGATION

Master's Thesis

Examiners: Professor Robert Piche,
Associate Professor Elena-Simona
Lohan
Examiners and topic approved by the
Faculty Council of the Faculty of
Computing and Electrical
Engineering on 4th June, 2014.

ABSTRACT

TAMPERE UNIVERSITY OF TECHNOLOGY

Master's Degree Program in *Electrical Engineering*

KHAN, MUHAMMAD WAQAS AHMAD: Statistical Sensor Fusion of Ultra Wide Band Ranging and Real Time Kinematic Satellite Navigation.

Master of Science Thesis, 46 pages, 00 Appendix page

November 2014

Major subject: *RF Electronics*

Examiners: Professor Robert Piche and Associate Professor Elena-Simona Lohan.

Keywords: Real Time Kinematic (RTK), Global Positioning System (GPS), Ultra-Wide Band (UWB), Kalman Filter (KF), Cycle Slip (CS), Integer Ambiguity (IA), Base Station (BS), Rover, Fusion.

Position, velocity and time (PVT) can be calculated from Global Positioning System (GPS). Two types of GPS measurement models are present, code phase measurement model and carrier phase measurement model. Range measurement in GPS is affected by different types of errors including atmospheric, multipath, satellite and receiver clock and ephemeris errors. Atmospheric errors are the biggest source of error amongst these.

Receivers within close proximity to each other face mostly same atmospheric errors from GPS signal. Several differential techniques have been developed during the last few years to mitigate these common errors. It means that the accuracy can be improved by using multiple receivers which mitigate the majority of errors. Real Time Kinematic (RTK) concept uses carrier phase measurements, which have high accuracy. RTK concept was originally developed for application such as surveying. The unknown ambiguity in the number of cycle between each satellite and receiver node is the main issue in RTK technique, moreover these ambiguities are integer numbers. Once the ambiguity is solved, it remains constant as long as the receiver maintains a phase lock on satellites signals. However, the loss of phase lock results in cycle slips and the ambiguity needs to solve again. In this work, RTKLIB, an open source software, is used for the RTK GPS positioning.

Ultra-Wide Band (UWB) is known since early 1900s with synonymous terms such as impulse, time domain, nonsinusoidal, baseband, carrier free, orthogonal function and large relative bandwidth radio signals. The huge frequency bandwidth of UWB makes it suitable for positioning and navigation applications. Multipath resistance, high accuracy, low cost and low power implementation are other features of UWB. The huge bandwidth in frequency domain corresponds to short pulse in time domain, usually of nanosecond (ns) order. The Time of arrival (TOA), the time difference of arrival (TDOA) and the received signal strength (RSS) are known methods to calculate the range between the source and the target through UWB. TOA and TDOA are highly accurate but have clock synchronization problem. To overcome this problem, a modified method known as two-way time-of-flight can be used. BeSpoon phone equipped with UWB is used here for UWB ranging.

To summarize the previous discussion, RTK GPS positioning has a high accuracy but has integer ambiguity resolution problem which causes cycle slips and requires good satellite visibility as well. Moreover RTK GPS positioning solution is for outdoor applications only and has high dynamic outdoor range. UWB, on the other hand, can give highly accurate positioning solution but has low dynamic range. UWB can be used for both indoor and outdoor applications. Moreover, high bandwidth of UWB makes it multipath resistant and as result can be used in shadow areas. Thus, the fusion of RTK GPS and

UWB positioning may compensate the limitations of both and result in better performance system. In this thesis a Kalman filter is used for fusion of UWB and RTK GPS positioning solutions.

UWB gives range from tags which are in meter and relative to BeSpoon phone while RTK GPS positioning solution is in geodetic coordinates form (latitude and longitude). Three steps are involved in fusion; first, convert UWB ranges to position in local coordinate by using trilateration, second, convert geodetic coordinates of RTK GPS to local coordinates through rotation matrix and third, use Kalman filter for fusion of both positioning data. The main goal of the thesis is the fusion of both RTK GPS and UWB positioning solutions with the help of Kalman filter in order to obtain better performance compare to stand-alone RTK GPS.

Tampere University of Technology (TUT) parking area is used for testing. One corner of TUT parking area has the known coordinate point which is used for the base station of RTK GPS. Reference track and tags positions are drawn through Laser instrument Leica TPS1200 which has millimeter level of accuracy.

Measurement results show that the fusion of UWB and RTK GPS positioning solutions have better performance compared to stand-alone RTK GPS solution. Whenever measurement from RTK GPS gives erroneous/missing result, the measurement from UWB sensor corrects it and the resulting solution from filter has better performance.

PREFACE

This Master of Science thesis is written in collaboration of Department of Electronics and Communications Engineering and Department of Automation Science and Engineering. This thesis is funded by Department of Automation Science and Engineering. The work I have done as research assistant is presented in this thesis.

I thank my supervisors Professor Robert Piche and Associate Professor Elena-Simona Lohan for their continuous support, guidance and valuable feedback. I also thank Hannu Kupila and Joonas Melin for providing necessary equipment. I would like to mention my research group members specially Simo Ali-Löytty, Helena Leppäkoski, Pavel Davidson, Henri Nurminen, Davide La Croce, Juha Ala-Luhtala, Ville Huttunen and Philipp Muller for their help.

I want to thank all my friends specially Shahbaz, Rao Uzair, Safdar, Rizwan and Haresh for their help during my measurements. I would like to thank my family for their continuous support to make this thesis possible.

Tampere November 10, 2014
Muhammad Waqas Ahmad Khan

Tampere, Finland.

TABLE OF CONTENTS

1. Introduction	1
1.1. Background	1
1.2. Thesis motivation	2
1.3. Research objective	2
1.4. Author contributions	3
1.5. Thesis outline	3
2. Theoretical background	4
2.1. Ultra-Wide Band (UWB)	4
2.1.1. UWB history	4
2.1.2. UWB signal definition	5
2.1.3. UWB ranging	9
2.1.4. Testing and results of BeSpoon phone UWB	12
2.2. Real Time Kinematic (RTK) GPS	13
2.2.1. RTK GPS background	15
2.2.2. RTKLIB	16
2.2.3. RTK GPS configuration	20
2.2.4. Testing and result	22
2.3. The Kalman filter for data fusion	22
2.4. Summary	25
3. UWB and RTK GPS fusion	26
3.1. UWB and RTK GPS fusion configuration	26
3.2. Kalman filter fusion parameters	30
3.3. Testing method	32
3.4. Summary	35
4. Results and discussion	36
4.1. Result with 6 UWB tags	36
4.2. Result with 4 UWB tags	38
4.3. Comparison of results	40
4.4. Summary	41
5. Conclusions and future work	42
5.1. Conclusions	42
5.2. Future work	43
References	44

LIST OF FIGURES

2.1	UWB signal definition.	6
2.2	UWB example pulse shape.	7
2.3	4 bits 1010 transmission through UWB signal.	7
2.4	ECC EIRP emission limits for UWB system without appropriate mitigation techniques[1].	8
2.5	ECC EIRP emission limits for UWB system with appropriate mitigation techniques[1].	8
2.6	Ranging through two-way time-of-flight method.	10
2.7	BeSpoon phone and six tags equipped with UWB.	12
2.8	Static line-of-sight error measurement (red *), linear regression line (continuous blue line) and 95% credibility interval limits (green dashed line).	13
2.9	Dynamic line-of-sight error measurement (red *), linear regression line (continuous blue line) and 95% credibility interval limits (green dashed line).	14
2.10	(a) Yuan10 USB receiver (b) ANN-MS u-blox active GPS antenna	17
2.11	RTKLIB GUI APs on windows 7 OS.	17
2.12	RTKNAVI main window.	19
2.13	RTKNAVI data flow.	19
2.14	RTK GPS configuration through serial connection.	20
2.15	RTK GPS configuration through WiFi.	21
2.16	RTK GPS configuration through internet.	21
2.17	RTK GPS configuration through NTRIP Caster.	21
2.18	RTK GPS configuration used in thesis.	22
2.19	Sample testing result of RTK GPS positioning.	23
2.20	Kalman filter recursive steps.	23
3.1	UWB and RTK GPS fusion properties.	27
3.2	UWB and RTK GPS fusion configuration in our measurements.	28
3.3	Sample UWB data of approximately 1sec from BeSpoon phone.	28
3.4	RTK GPS + UWB fusion process flow.	29
3.5	Fusion filter algorithm.	31
3.6	Photo of a known coordinate point.	32
3.7	Google Earth view of testing setup. Parking is approximately 100m long and 30m wide.	33
3.8	Front view of testing setup.	34
3.9	Cart.	34
3.10	Base station.	35
4.1	Result with six UWB tags.	37
4.2	Track is divided into three sub tracks.	37

4.3	Result with cycle slip (simulated).	39
4.4	Result with four UWB tags second scenario.	39
4.5	Result with four UWB tags third scenario.	40
5.1	Proposed hexacopter navigation system configuration for future studies. . .	43

LIST OF TABLES

2.1	Ranging error calculation with different oscillator errors.	10
2.2	Comparison between BeSpoon Phone and Zebra Technologies Dart RTLS UWB.	11
2.3	Measurement errors for single frequency (L1) receiver [2].	15
2.4	RTKLIB functions and GUI APs [3].	18
2.5	Discrete Kalman filter equations summary.	25
3.1	Coordinate detail of surveyed point.	32
4.1	RMS error (m) comparison of RTK GPS, UWB and fusion of UWB and RTK GPS results.	38
4.2	RMS error (m) comparison of fusion results with and without cycle slip of sub track 2	38
4.3	RMS error (m) comparison of RTK GPS, UWB and fusion of UWB and RTK GPS results with 4 tags	38
4.4	RMS error (m) comparison of RTK GPS, UWB and fusion of UWB and RTK GPS results with 4 and 6 tags	41

LIST OF SYMBOLS AND ABBREVIATIONS

GPS	Global Positioning System
PRN	Pseudo-Random Noise
RTK	Real Time Kinematic
UWB	Ultra-Wide Band
TOA	Time Of Arrival
TDOA	Time Difference Of Arrival
RSS	Received Signal Strength
KF	Kalman Filter
BS	Base Station
WAAS	Wide Area Augmentation System
INS	Inertial Navigation System
CS	Cycle Slip
FCC	Federal Communications Commission
SNR	Signal-to-Noise Ratio
TH	Time Hopping
IF	Intermediate Frequency
EIRP	Effective Isotropic Radiated Power
ppm	Parts-Per-Million
RHCP	Right Hand Circular Polarization
GUI	Graphical User Interface
AP	Application Program
PC	Personnal Computer
APK	Android Application Package
x	State Vector
\hat{x}	Estimated State Vector
$x_k(-)$	Priori value of State Vector at epoch k
$x_k(+)$	Posteriori value of State Vector at epoch k
F	Dynamic Matrix
Q	Noise Covariance Matrix or System Noise Matrix
w	Dynamic Noise Matrix
H	Observation Matrix
v	Measurement Noise Matrix
R	Noise Covariance Matrix or Measurement Noise Matrix
$P_k(-)$	Error Covariance Matrix at epoch k
K	Kalman Gain Matrix
$P_k(+)$	Updated Error Covariance Matrix at epoch k
z	Input Measurement Matrix
σ	Standard Deviation

1. INTRODUCTION

1.1. Background

In 1960s Global Positioning System (GPS) was established and presently it is fully functional to calculate position, velocity and time. The satellite constellation normally consists of enough NAVSTAR satellites orbiting in six different orbital planes such that at least 4 satellites are visible from anywhere on the Earth. Each satellite transmits signal on several L band frequencies. Two of them are L1 and L2 signals. L1 signal center frequency is 1575.42 MHz, while L2 signal center frequency is 1227.60 MHz. Moreover, in March 2009, an L5 signal was included with the center frequency 1176.45 MHz. GPS can serve unlimited number of users because the receivers act as passive element. Moreover GPS uses one-way time-of-arrival (TOA) method for ranging. [2], [4]

GPS is affected by different types of errors including atmospheric, satellite and receiver clocks, multipath and ephemeris errors. Since last few years, several differential techniques have been developed to mitigate the common errors between two GPS receivers close to each other. There are three basic types of augmentations to GPS. The first type requires that an information related to the additional error is transmitted. The Second type is based on the transmission of raw information. The third type requires the additional transmission of other navigational information from other systems/sensors, such as velocity, acceleration, etc.

The Wide Area Augmentation System (WAAS) developed by Federal Aviation Administration (FAA), the European Geostationary Navigation Overlay System (EGNOS) developed by European Space Agency, the European Commission and EUROCONTROL, the Multifunction Satellite Augmentation System (MSAS) developed by Japanese and the GPS Aided GEO Augmented Navigation (GAGAN) developed by Indian government are few systems that transmit correction to users for removing errors. Real Time Kinematic (RTK) technique transmits raw data from base station to the user (rover) to remove errors. Systems including Compass (heading aiding), Inertial Navigation System (INS), high-stability clocks, terrain mapping/corrections, star tracking and VHF Omni-directional Ranging (VOR) transmit different types of information used to remove errors. [5]

GPS uses two types of measurement models: the code phase measurements and the carrier phase measurements. The carrier phase measurements give good accuracy compared to code phase measurements but suffer from the cycle slips (CS) problem, because of multipath and satellite visibility issues. The Real Time Kinematic (RTK) GPS uses carrier phase measurements and gives centimeter level of accuracy. In order to maintain centimeter

level accuracy system, one should be able to overcome cycle slips problem which can be achieved through augmentation of some other system input.

1.2. Thesis motivation

RTK was originally developed for applications such as surveying; in our case the target application is the tracking and the control of a robot hexacopter. A hexacopter is a member of multi-rotor flying devices which consist of multiple fixed rotors attached to a simple mechanical construction and it is used in many various applications such as aerial mapping and photography, power line inspections, crop control, law enforcement surveillance, etc. The main issue in RTK is the determination of the number of cycles, called integer ambiguity, between the receiver and each satellite. Once the ambiguity is solved, it remains constant as long as the receiver maintains a phase lock on the satellite signals. However, the hexacopter maneuvers or the satellite visibility obstructions can cause the loss of phase lock, and the integer ambiguity needs to be solved again. This can take several seconds, during which the RTK positioning accuracy is severely degraded. To ensure continuous high-accuracy positioning, complementary positioning signals are needed. This motivates the fusion of UWB ranging and RTK GPS positioning through loosely coupled approach in Kalman filter (KF).

Ultra-Wide Band (UWB) uses two-way time-of-flight method for ranging and gives centimeter level of range accuracy. Multipath resistance, high accuracy, low cost and low power implementation makes UWB a good candidate for augmentation to RTK GPS to overcome cycle slips problem. References [6] and [7] show that improvement in DGPS positioning can be achieved through tightly coupled approach in a Kalman filter (KF). In tightly coupled approach, the measurements from different systems are combined together to input a joint estimator. Similarly, the pseudorange from RTK GPS receiver and with the range from UWB are input to combine estimation method. But in our case we are using position coordinates from RTK GPS and position from UWB (position from UWB ranging is calculated) for which loosely coupled approach is good option. Reference [8] shows improvement in cycle slips problem in Real time Kinematic (RTK) GPS through integrating UWB ranging into C-LAMBDA method. BeSpoon phone equipped with UWB ranging, which has 80m range, is used along with RTKLIB, open source software tool, for RTK GPS positioning solution. Low cost GPS carrier phase receiver Yuan10, consists of Skytraq S1315F-RAW chip, has been used.

1.3. Research objective

The research objective of the thesis is to overcome the Real Time Kinematic (RTK) GPS cycle slips problem by augmenting with Ultra-Wide Band (UWB) ranging. The fusion of UWB and RTK GPS is achieved through Kalman filter. In this thesis, the loosely coupled approach is used with RTK GPS update rate of 1Hz and UWB ranging update rate of 4Hz.

1.4. Author contributions

The major contributions of this thesis are:

1. Analyze UWB range measurement accuracies of BeSpoon phone.
2. Fusion of UWB ranging and RTK GPS positioning solutions through loosely coupled approach.
3. Post processing of measurement data to analyze effect on fusion results of UWB tags number and their placement.
4. Literature review of RTK GPS, UWB and Kalman filter.
5. Setup the measurements environment and performing the measurements.
6. Analysis and interpretation of obtained results.

First three are the novel contribution of the thesis.

1.5. Thesis outline

The rest of the thesis consists of four chapters. Chapter 2 contains the history, definition and ranging method of UWB. It also includes a description about RTK GPS and RTKLIB software tool. At the end of this chapter a short Kalman filter overview is provided. Chapter 3 provides the details about the methods and materials used in the thesis. The used configuration of the overall system setup and the Kalman filter parameter settings are explained. Chapter 4 presents the obtained results of the thesis. The conclusion and the work related to future are provided in Chapter 5.

2. THEORETICAL BACKGROUND

The fact that Ultra-wide band has a high bandwidth makes it a good candidate for navigation applications, due to its high positioning accuracy both indoor and outdoor. Real time Kinematic GPS, on other hand, gives a good accuracy for outdoor positioning problem but has cycle slips problem.

In this chapter, the brief history, definition, ranging technique and testing results of UWB equipped BeSpoon phone are presented. After this, RTK GPS background along with some details about an open source tool, RTKLIB, and different possible configurations for RTK GPS are presented. At the end of chapter, the Kalman filter is explained in some details. All these concepts are basis of this thesis.

2.1. Ultra-Wide Band (UWB)

The huge frequency bandwidth of UWB makes it suitable for positioning and navigation applications. The huge bandwidth, multipath resistance, high accuracy, low cost and low power implementation are features of UWB.

Broadly, the UWB can be divided into two types [6]:

- Impulse based UWB, which transmit short pulses by utilizing complete frequency band, for example short Gaussian pulses.
- Multicarrier based UWB, which transmit signals by multicarrier methods, for example orthogonal frequency division multiplexing (OFDM).

The UWB equipment used in this thesis is impulse based (BeSpoon phone [9]). Due to this only impulse based UWB is considered in detail throughout this thesis and whenever UWB is used it refers to impulse based UWB unless otherwise specified. The reader interested in multicarrier based UWB is directed to chapter 2 of [1] for more details. UWB history, definition and ranging methodology are explained further.

2.1.1. UWB history

The UWB is known since early 1900s with synonymous terms such as impulse, time domain, nonsinusoidal, baseband, carrier free, orthogonal function and large relative bandwidth radio signals. But pioneer contribution in developing UWB is from Harmuth of Catholic University of America, Ross and Robbins from Sperry Rand Corporation, Paul van Etten from the US Air Force and Russian researchers in early 1960s [10]. The US

patent by Ross can be considered as main milestone in UWB communications [11]. The main components required to build UWB systems, explained by early 1970s, includes:

- Pulse train generator.
- Pulse train modulator.
- Switching pulse train generator.
- Detection receiver.
- Wide-band antennas.

All of these components are well known and available in market in 1975. A complete UWB system could be built easily by purchasing these components in late 1970s. Even today, overall system components, explained above, are the same with subsystem level changes due to improvement/change of technology [10].

UWB term was first time used by US department of defense in 1989 which is result of workshop organized by Col. J.D. Taylor in which over 100 participants were welcomed. Since that date, China and Russian Federation made substantial progress in UWB [10]. US Federal Communications Commission (FCC), in 2002, released the unlicensed 7.5GHz band which brought UWB in spotlight [12]. In 2005, US Federal Communication Commission (FCC) released Second Report which amended part 15 according to which permission to use peak emission power is given [13]. Both of these documents provide appropriate definition for UWB signal.

2.1.2. UWB signal definition

UWB signal can be defined in term of absolute or relative bandwidth. In term of absolute, signal with at least 500MHz of bandwidth is known as UWB signal while as relative, signal with 20% fractional bandwidth is known as UWB signal. Both of these definitions are in accordance to US FCC [12]. Absolute bandwidth (B_{obs}) is the difference of higher (f_H) and lower (f_L) frequencies which are at relatively -10dB below to peak emission power as shown in Figure 2.1 and is given by

$$B_{obs} = f_H - f_L \quad (2.1)$$

the fractional bandwidth, on other hand, can be defined as

$$B_{frac} = \frac{B_{obs}}{f_c} \quad (2.2)$$

where f_c , which is center frequency, is given by

$$f_c = \frac{(f_H + f_L)}{2} \quad (2.3)$$

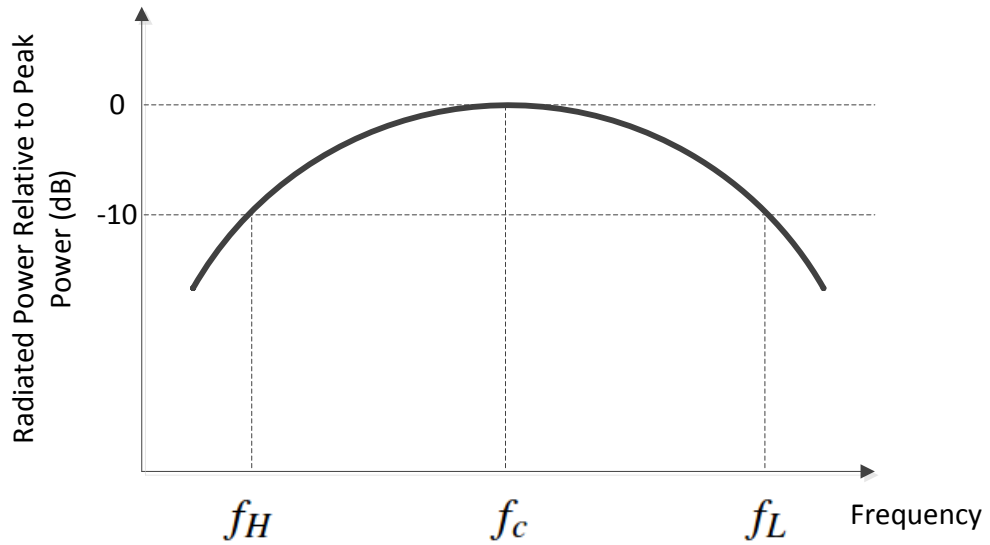


Figure 2.1. UWB signal definition.

Putting the values of B_{obs} and f_c into equation (2.2), this gives the fractional bandwidth as

$$B_{frac} = \frac{2(f_H - f_L)}{(f_H + f_L)} \quad (2.4)$$

Equations (2.1) and (2.4) are mathematical form of absolute and relative UWB bandwidth definitions respectively.

The pulse shape in UWB system can be derivative of Gaussian pulses, modified Hermit polynomials and wavelet pulses [1]. An example of a second derivative Gaussian pulse is plotted in Figure 2.2. The information in UWB system is transferred through position and polarity of the pulse. Each pulse occupy specific interval known as frame. To avoid collisions with other UWB pulses, position of pulse within frame is determined by time hopping (TH) code [1]. For example in Figure 2.3, UWB system transmits 4 bits 1010. Each bit consists of two pulses and polarity of pulse determines whether it is 1 or 0 bit (BPSK). Each frame (T_f) consists of $3T_C$, where T_C represents chip interval. For the first bit TH is $\{0, 1\}$, as first pulse is transmitted at zero T_C second while second is transmitted at one T_C second.

The shannon capacity law states that with the increase of bandwidth of signal, more information can be transferred with same signal-to-noise ratio (SNR). Due to the pulse transmission in UWB, the power consumption of system reduces which increase battery life of the system along with reduction of interference to other systems using the same frequency band. Moreover pulse transmission feature of UWB makes it possible to transmit signal without any sine-wave carrier and as a result no intermediate frequency (IF) processing is required.[1]

As stated previously, the UWB is using huge frequency band and as a result, UWB

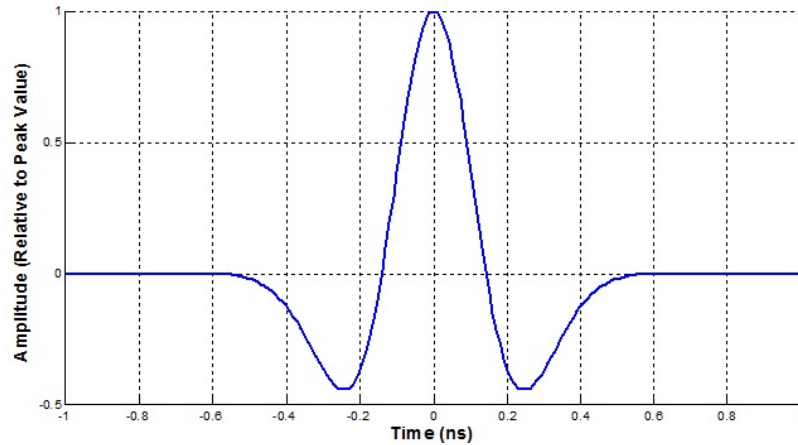


Figure 2.2. UWB example pulse shape.

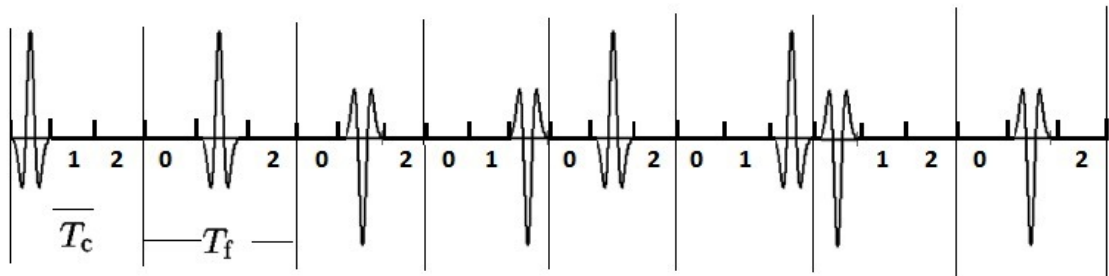


Figure 2.3. 4 bits 1010 transmission through UWB signal.

needs to coexist with other systems without creating interference to other systems. To avoid such interference problem some limit to maximum power emission from UWB need to be imposed [1]. The limit imposed by US FCC to effective isotropic radiated power (EIRP) in any direction is based on UWB application. For indoor usage, for outdoor usage, in vehicular radar system and in imaging systems, EIRP level limit varies with frequency band but maximum allowable limit in any scenario must not exceed -41.3 dBm/MHz. The reader interested in US FCC power level limits can read reference [1] or [12] for more details. Other regulatory authorities that impose limits to EIRP level from UWB system include Electronic Communications Committee (ECC) in Europe and Ministry of Internal affairs and Communications (MIC) in Japan. But maximum limit to EIRP level from UWB system in any scenario is -41.3 dBm/MHz for both regularities as well [1]. Figure 2.4 shows ECC EIRP level limits for UWB system without appropriate mitigation techniques and Figure 2.5 shows ECC EIPR level limits for UWB system with appropriate mitigation techniques. BeSpoon Phone [9] used in this thesis has 500 MHz band with center frequency 3.9936 GHz and has maximum EIRP level below -41.3 dBm.

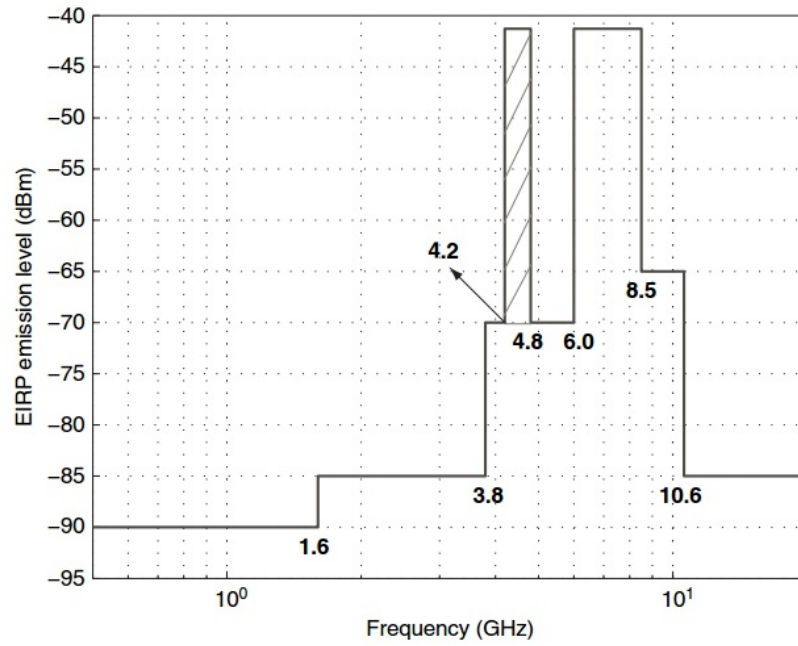


Figure 2.4. ECC EIRP emission limits for UWB system without appropriate mitigation techniques[1].

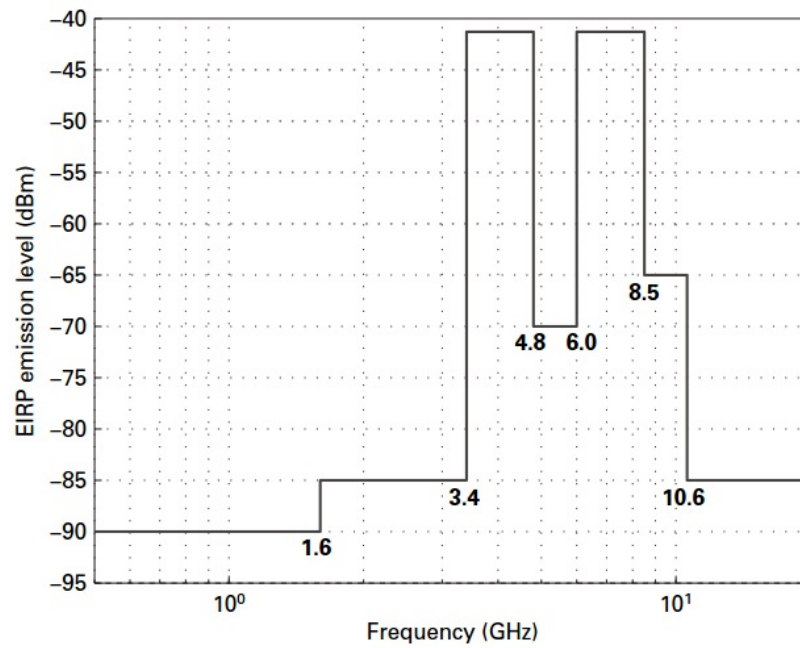


Figure 2.5. ECC EIRP emission limits for UWB system with appropriate mitigation techniques[1].

2.1.3. UWB ranging

Time of arrival (TOA), time difference of arrival (TDOA) and received signal strength (RSS) are known methods to calculate the range between the source and the target through UWB. A short description of each method is as following: [1], [14], [15]

- Time of arrival (TOA) calculates the range between the source and target by multiplying the time taken by signal to propagate from source to target with the speed of light. This requires clock synchronization between the source and target or some means to share clock information between them. Accuracy of TOA is high but the disadvantage is the clock synchronization requirement both between the sources and between the source and the target.
- Time difference of arrival (TDOA) calculates the range difference between the source and the target by time difference of signal arrival at synchronized targets. This does not require the source and the target clock synchronization. TDOA has high accuracy and is less complicate as compared to TOA. Disadvantage includes clock synchronization between targets.
- Received signal strength (RSS) calculates the range from received signal strength at the target. It is assumed that transmitted power from the source is known along with the signal propagation model. RSS is easy to implement but is less accurate.

TOA and TDOA are highly accurate but require clock synchronization. To bypass this requirement, a modified method known as two-way time-of-flight can be used. Two-way time-of-flight method, shown in Figure 2.6, can be performed in five steps: [6], [9]

- The source sends the message to the target and start its chronometer.
- When signal arrived at the target, the target starts its own chronometer.
- After processing the message, the target replies (the message contains processing time information as well) and stops its chronometer.
- After message is received by the source, the source stops its chronometer (this is total transaction time).
- The range is calculated from

$$Range = \frac{Speed\ of\ Light * \{Total\ Transaction\ Time - Processing\ Time\}}{2} \quad (2.5)$$

The processing time is usually greater than the flight time because it takes time to include necessary information that facilitates ranging measurement. Frequency offset created due to the source and the target oscillator difference is the main cause of error in UWB ranging. Detail discussion on this issue is in IEEE 802.15.4a standard [16]. Reference [6] derived the formula to the flight time error estimation due to oscillator frequency offset problem and is given as

$$\epsilon_f \approx e_A t_f + \frac{1}{2}(e_A - e_B)t_p \quad (2.6)$$

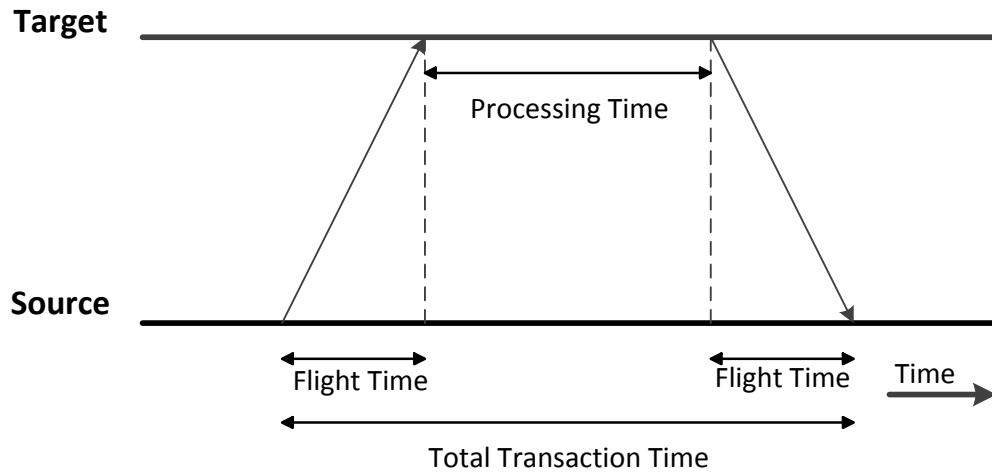


Figure 2.6. Ranging through two-way time-of-flight method.

where ε_f estimated flight time error, e_A error due to the source oscillator (it is measured in parts-per-million(ppm)), e_B error due to the target oscillator (it is also measured in ppm), t_f is the flight time and t_p is the processing time. Table 2.1 shows two examples with different oscillator errors. It is clear that by keeping rest of the things same, error due to oscillators have large contribution to the ranging error.

Table 2.1. Ranging error calculation with different oscillator errors.

Example 1	Example 2
$t_f = 0.333\mu s$	$t_f = 0.333\mu s$
$t_p = 200\mu s$	$t_p = 200\mu s$
$e_A = 20$ ppm	$e_A = 5$ ppm
$e_B = -20$ ppm	$e_B = -5$ ppm
$\varepsilon_f = 0.400666$ ns	$\varepsilon_f = 0.200166$ ns
Ranging Error= 1.201 m	Ranging Error= 0.6 m

Figure 2.7 shows the Bespoon phone and six tags used in the thesis. Bespoon phone is using two-way time-of-flight method for ranging. The Department of Signal Processing of Tampere University of Technology (TUT) has also a Zebra Technologies Dart Real Time Locating System (RTLS) based on short pulse UWB technology. A comparison between Bespoon Phone and Zebra Technologies Dart RTLS is presented in Table 2.2 [9], [17]. Only BeSpooon phone is used in this thesis, Zebra Technologies Dart RTLS is presented here just for comparison with Bespoon phone in term of cost, weight, technology etc.

A side note, the main differences between UWB based radar and conventional narrow-band radar are the changes of signal shape and antenna pattern dependency. By signal shape we mean the change of signal with time. The conventional radar has sinusoidal

Table 2.2. Comparison between BeSpoon Phone and Zebra Technologies Dart RTLS UWB.

	BeSpoon Phone	Zebra Technologies Dart RTLS
Technology	Pulse based UWB.	Pulse based UWB.
	Gives only relative range between Bespoon phone and tags.	Gives 2D, 3D location of tag in fixed environment and range of tags as well.
System	Complete system consists of Normal handheld Bespoon phone and tags.	Complete system consists of Dart RTLS Hub, Dart RTLS sensors and DartTags.
Ranging Technique	Asynchronous ranging.	Synchronous ranging.
Update Rate	Fixed update rate of 4Hz	Variable update rate 1-50Hz
Accuracy	Few cm (I have noticed 10 cm accuracy on average).	Around 10cm (4 inch) with signal averaging and 30cm (1 foot) without signal averaging.
Weight	Bespoon phone weight is 130gm.	Dart RTLS Hub weight is 1.64Kg.
UWB Antenna	Low gain UWB antenna installed at Bespoon phone with -3dBi gain.	Variable gain UWB sensor antenna option available from directional (14dBi) to omnidirectional (4.5dBi).
Range	300m range in ideal condition (according to specification) but I have noticed 80m range.	Range depends on sensor antenna type max range with directional antenna is 304.8m (1000 feet).
Dimensions	Bespoon phone is 13.2 cm x 6.6 cm x 0.98 cm.	Dart RTLS Hub is 35.6 cm x 22.9 cm x 8.9 cm.
Operating System	Android operating system installed on Bespoon phone.	Linux operating system installed on Dart RTLS Hub.
Cost	Around 500 euros.	Around 30000 euros.
Center Operating Frequency	3.9936GHz with 500MHz bandwidth.	6.55GHz with 500MHz bandwidth.



Figure 2.7. BeSpoon phone and six tags equipped with UWB.

waveform whose shape remains almost same while in case of UWB based radar signal shape changes at different stages and after reflection from different objects. Due to this problem it is difficult to work with UWB based radar especially in signal processing unit of the system. [18]

2.1.4. Testing and results of BeSpoon phone UWB

To assess the ranging error behavior of the BeSpoon phone UWB, both static and dynamic testings are performed. After measurements, the data is processed and linear regression line with 95% credibility interval limits is drawn [19] to check bias and variance dependency to distance.

A static line-of-sight testing was performed in an open area near Tampere University of Technology (TUT). BeSpoon phone was placed on fixed location and tags were moved on twelve different points starting from 5m to 60m with 5m difference. Laser instrument Leica TPS1200 [20] was used to locate twelve points with millimeter level of accuracy. Tracking mode is used to track the prism automatically. To collect the measurement, a tag was placed at desired location for few seconds. Seven independent measurements for each tag were collected. Figure 2.8. represents the error in each measured value, the linear regression line and 95% credibility interval limits.

The dynamic line-of-sight testing was performed by keeping the BeSpoon phone at fixed point and tags were moved on straight line. The straight line of length 35m started from 10m distance and ended at 45m distance from the BeSpoon phone. Lase instrument Leica TPS1200 [20] was used to draw the straight line. Constant velocity of 1 m/s is used for movement. The methodology adopted for the measurement is as following:

- Tags were moved on the straight line with known constant velocity.
- While moving, the range data on BeSpoon phone was stored and transferred to laptop after each round.
- Fifteen independent measurements for each tag were collected.

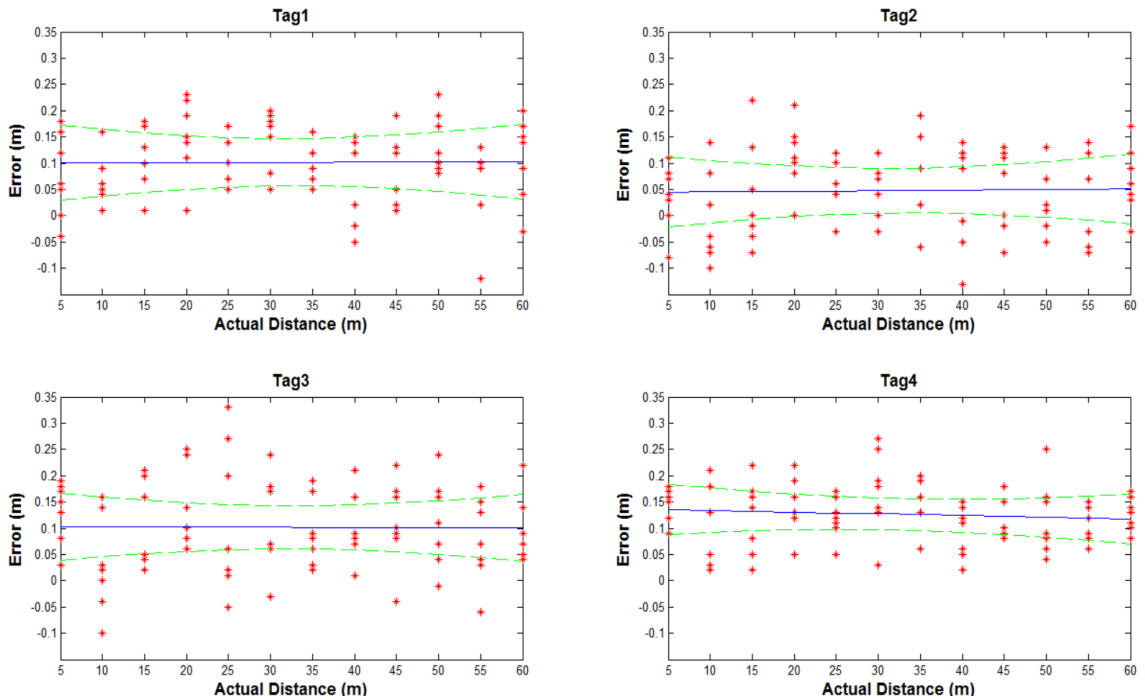


Figure 2.8. Static line-of-sight error measurement (red *), linear regression line (continuous blue line) and 95% credibility interval limits (green dashed line).

- The data was post processed after completion of all measurements.
- From known velocity, the time taken to cover each 5m of distance is calculated and range sample of that interval is extracted. For example, if velocity is 1m/s, to cover 5m distance required time will be 5 seconds. It means that the data is sampled after each 5 seconds to get measured range at 5m, 10m, and so on.

Figure 2.9. represents error in each measured value, linear regression line and 95% credibility interval limits. It appeared that all tags have approximately the same positive bias of 10cm and approximately same standard deviation of 10cm. Moreover it can be concluded that bias and standard deviation are independent of distance. This bias of 10cm is taken care of in the fusion filter.

2.2. Real Time Kinematic (RTK) GPS

US Navy and Air force each developed space-based navigation system in late 1960s. Eventually, both systems were combined into GPS. Within few years after that, 24 NAVSTAR satellites were orbiting in six different orbital planes such that at least 4 satellites were visible from anywhere on the Earth. Position, velocity and time (PVT) can be calculated from GPS. Each satellite transmit signal on several L band frequencies. Two of them are L1 and L2 signals. L1 signal center frequency is 1575.42 MHz while L2 signal center frequency is 1227.60 MHz. Moreover, in March 2009, L5 signal has been included with center frequency 1176.45 MHz. [2], [8]

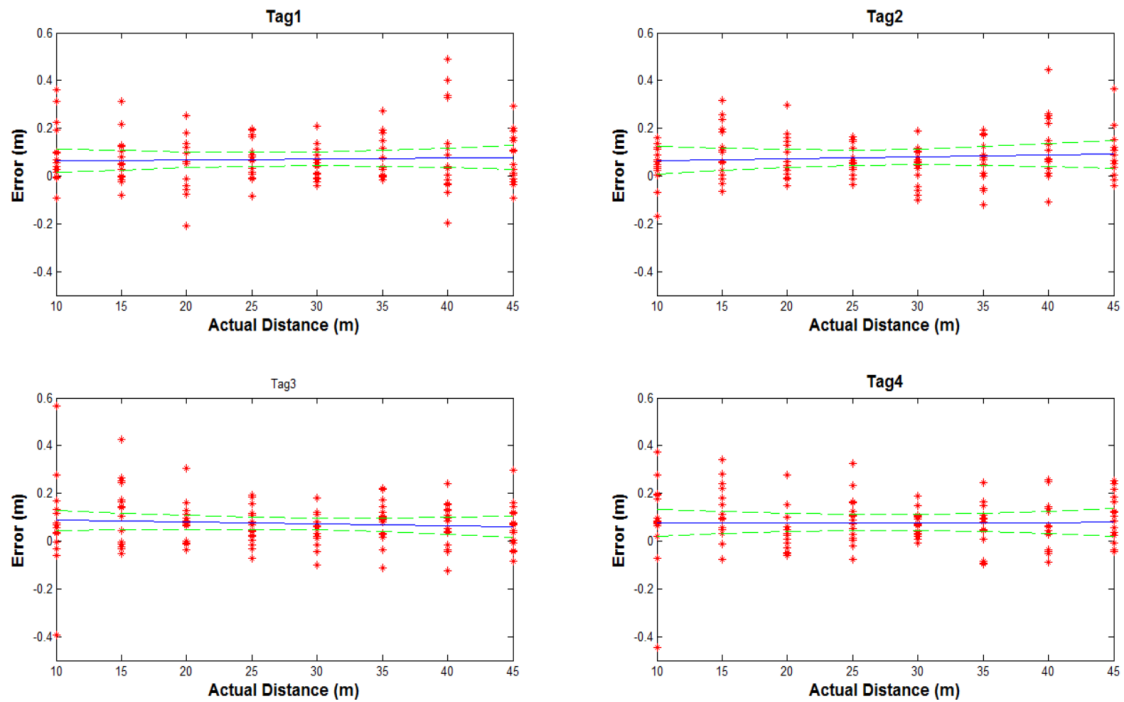


Figure 2.9. Dynamic line-of-sight error measurement (red *), linear regression line (continuous blue line) and 95% credibility interval limits (green dashed line).

GPS carrier signal is modulated with several codes which are known as pseudo-random noise (PRN) sequences. One code is known as C/A code (Clear/Coarse Acquisition) which is available for civilian use. Another code is known as P(Y) and also called protected code, which is for military use. The chip rate for C/A is 1.023 MHz (Megachips per second) while for P(Y) it is 10.23 MHz which is ten times more. A third code known as navigation message contains the ephemeris data which repeats every 30 seconds and the almanac data which repeats every 12.5 minutes. The ephemeris data contains clock drift, clock bias parameters and current health status of satellite while the almanac data contains information that allow the user to estimate all satellite positions in constellation. [2], [8]

Two types of GPS measurement models are present:

- Code Phase Measurement and
- Carrier Phase Measurement.

In the code phase measurement model, the GPS receiver makes the basic measurement from time taken by the signal to travel from the satellite to the receiver. As shown in Reference [2], the user equivalent range error (UERE) is typically about 1% of the signal's wavelength. The code wavelength is 293.1m which indicates that approximately 2.931m error is expected in measurement based on the code phase. In the carrier phase measurement, the GPS receiver makes measurement from difference of the carrier phase generated at receiver and satellite at the measurement instant. The carrier signal has wavelength of 19.05cm which means, an error of approximately 2mm is expected from the carrier phase measurement. [2]

The range measurement in GPS is affected by different types of errors. Major errors include:

- Atmospheric Errors
- Multipath errors
- Satellite and receiver clock errors and
- Ephemeris errors.

Atmospheric errors are among the biggest sources of error. Table 2.3 presents typical measurement errors for single frequency (L1) GPS receiver and user equivalent range error (UERE). [2]

Table 2.3. Measurement errors for single frequency (L1) receiver [2].

Source of error	RMS range error
Satellite clock and ephemeris	≈ 3 m
Atmospheric	≈ 5 m
Receiver noise and multipath	≈ 1 m
UERE	≈ 6 m

2.2.1. RTK GPS background

As stated previously, the largest source of error in GPS range measurement comes from atmospheric effects. Receivers within close proximity to each other face mostly same atmospheric errors from the GPS signal. Accuracy can be improved by using multiple receivers which mitigate majority of the errors. [2], [8]

Several differential techniques are present, some of them includes:

- Satellite Based Augmentation System (SBAS).
- Wide Area Augmentation System (WAAS).
- Wide Area GPS Enhancement (WAGE).
- Ground Based Augmentation System (GBAS).
- Differential GPS (DGPS) and
- Real Time Kinematic (RTK) GPS.

Real Time Kinematic GPS details will be presented here, for the rest, the reader is referred to [2].

Real Time Kinematic uses carrier phase measurements, which has high accuracy, and was originally developed for application such as surveying. As stated in the previous section, millimeter level accuracy can be achieved with carrier phase measurements; however there is one complication to solve integer ambiguity is involved. The unknown ambiguity in cycle between each satellite and receiver node is the main issue in RTK

technique, moreover these ambiguities are integer numbers and usually represented by N . Once the ambiguity is solved, it remains constant as long as receiver maintains a phase lock on satellites signals. However, a loss of phase lock results in cycle slip and ambiguity needs to be solved again. [2], [8] The loss of phase lock happens very often in locations with bad satellite visibility and in shadow regions such as forest, streets etc.

The technique used by RTK is as follows:

- Ground base station is placed on well-known/surveyed location.
- Transmission link between base station and rover is established through radio, wire or through any other means.
- Ground base station and rover are both able to receive carrier phase measurement from GPS signal.
- Real time measurement from base station is sent through transmission link to rover.
- Rover calculates its position through difference from base station measurement and its own measurement by mitigating common errors between two.

One thing need to be highlighted here: terms ‘base station’ and ‘rover’ vary from literature to literature, for example Misra and Enge 2006 uses ‘reference station’ instead of ‘base station’. The reason why these terms are used here is: RTKLIB (explained in next section) uses these terms and it is easily to correlate results in further chapters if same terms are used here.

The carrier phase receiver, for both base station and rover, used in thesis includes Yuan10 receiver of OneTalent GNSS and ANN-MS u-blox active GPS antenna. Yuan10, shown in Figure 2.10(a), is USB serial receiver consists of Skytraq S1315F-RAW GPS and regular female RF connector. It has a tracking sensitivity of -161 dBm, power consumption less than 150mW and variable update rate up to 20Hz [21]. The ANN-MS u-blox antenna, shown in Figure 2.10(b), is an active antenna of L1 frequency band, consists of amplifier with gain 27dB and noise figure 1.8dB. The antenna has 4dBi peak gain, 10MHz bandwidth, maximum 2 VSWR and right hand circular polarization (RHCP) [22].

Yuan10 receiver does not require any special driver to connect with computer and the data can be evaluated easily through freely available software such as RTKLIB.

2.2.2. RTKLIB

RTKLIB is an open source freely available software package specifically designed for applications of real time and post process positioning. The package contains portal program library and application programs executable on windows and source code for compilation to run on other operating systems. Table 2.4 shows different functions and graphical user interface (GUI) application program (AP) names included in RTKLIB software package while Figure 2.11 shows graphical representation of these GUI APs on windows 7 operating system. [3]

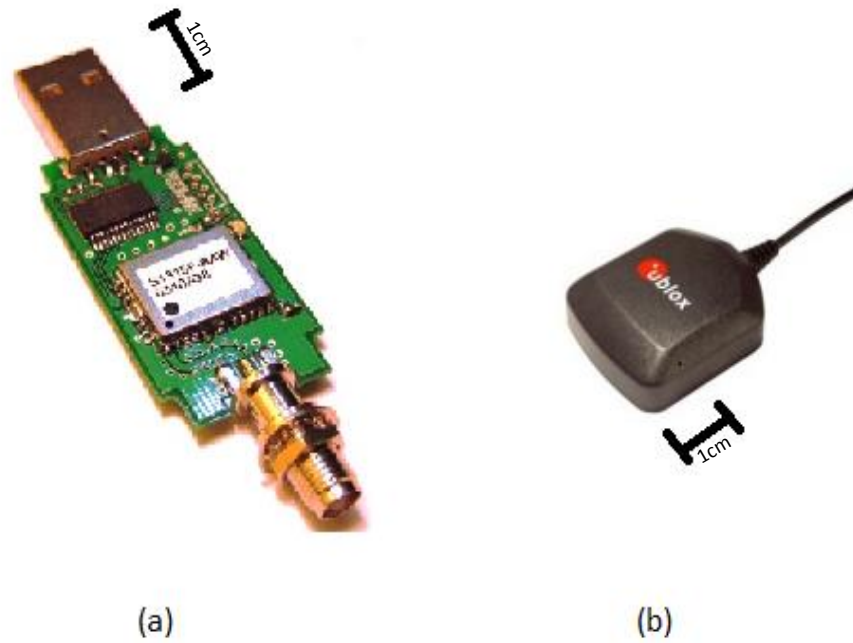


Figure 2.10. (a) Yuan10 USB receiver (b) ANN-MS u-blox active GPS antenna

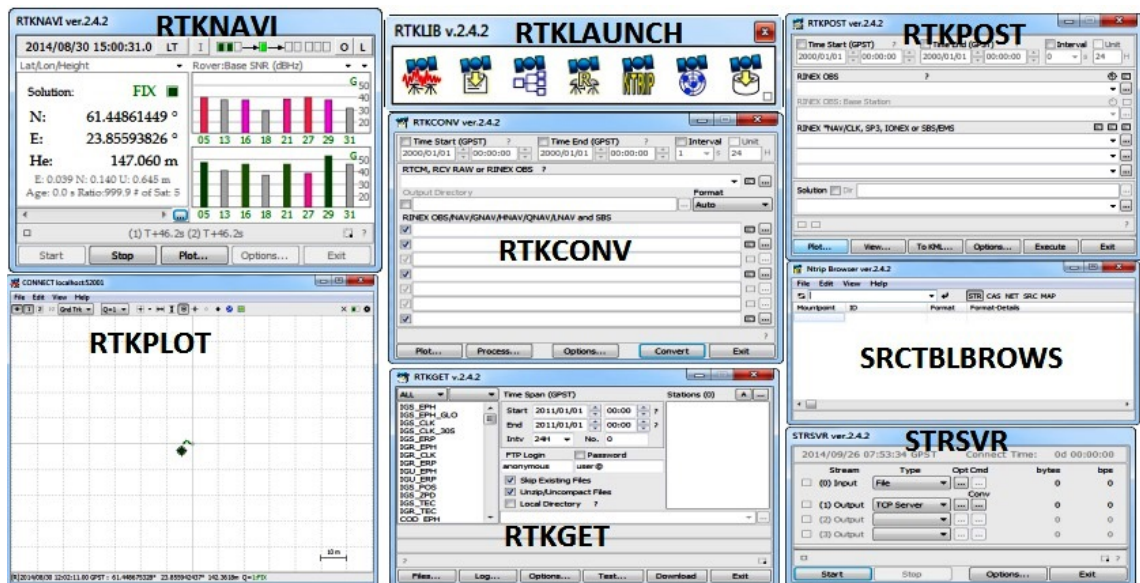


Figure 2.11. RTKLIB GUI APs on windows 7 OS.

Table 2.4. *RTKLIB functions and GUI APs [3].*

Function	GUI AP
Application program launcher	RTKLAUNCH
Real Time Positioning	RTKNAVI
Communication server	STRSVR
Post processing analysis	RTKPOST
RINEX converter	RTKCONV
Plotting of solutions and observation data	RTKPLOT
Downloader for GNSS products and data	RTKGET
NTRIP browser	SRCTBLBROWS

RTKLIB is in process of continuous update and this thesis uses latest available version 2.4.2. For further studies, it is better to check latest available update at [23]. RTKLIB supports:

- GPS, GLONASS, Galileo, QZSS, BeiDou and SBAS.
- Real time as well as post processing of positioning solutions.
- Various GNSS positioning modes including Single, DGPS, Kinematic, Fix, Static, Moving baseline, PPP kinematic/static/Fix.
- Various GNSS formats and receivers, details can be found in [3].
- Various external transmission links including serial, TCP/IP, NTRIP, log files and FTP/HTTP.

This thesis uses RTKNAVI, RTKPLOT and STRSVR APs of RTKLIB. A detail of these APs is presented here, for rest see [3]. RTKNAVI receive raw data from GPS receivers, process it in real time and display/store the output results. RTKNAVI involves following settings:

- Input settings for both base station and rover. Input raw data can be obtained through serial port, TCP client/server, NTRIP client and from stored log files.
- Output settings for solutions after process of raw data. Two types of solutions can be stored/sent at the same time. Output data can be sent through serial port, TCP client/server, NTRIP client or stored in log files. Output solution can be stored in many formats including lat/long/height, X/Y/Z-ECEF, E/N/U-baseline and NMEA0183.
- Raw data from receivers can be stored as log stream file or sent through serial port, TCP client/server, NTRIP client for later process.
- Overall settings including base station position coordinates, positioning mode etc also need to set through RTKNAVI.

Figure 2.12 shows main window of RTKNAVI while Figure 2.13 shows the data flow in RTKNAVI from input to output and log stream. RTKPLOT AP is used to plot the results

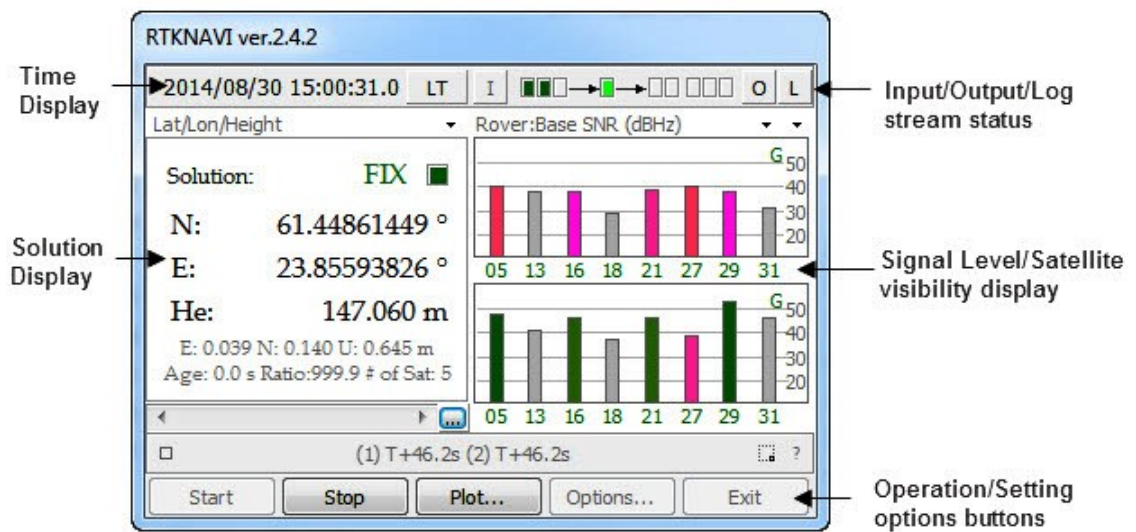


Figure 2.12. RTKNAVI main window.

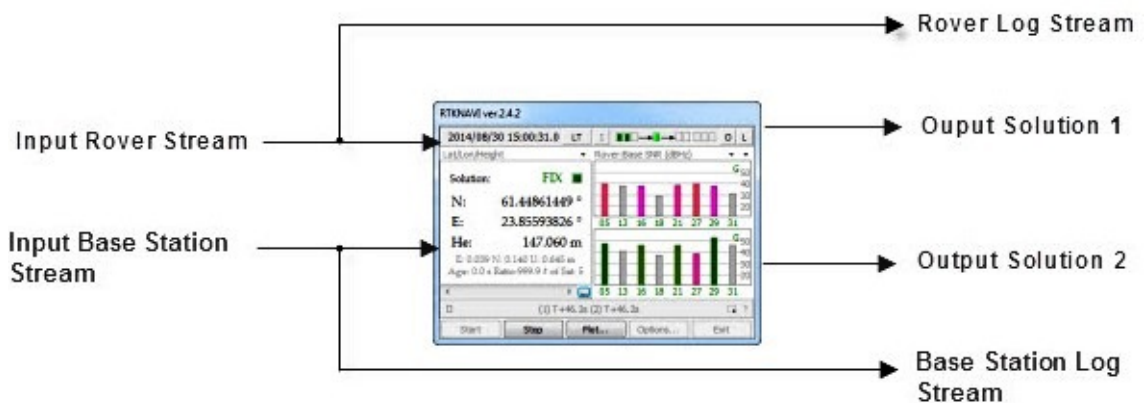


Figure 2.13. RTKNAVI data flow.

obtained after processing. STRSVR AP helps to make transmission link between base station and rover. Settings for input and output of STRSVR are the same as explained in RTKNAVI.

Related to RTK positioning, RTKLIB provides three types of solutions [3]:

Fix: solution is carrier based relative positioning and integer ambiguity is properly resolved.

Float: solution is carrier based relative positioning and integer ambiguity is not resolved properly.

Single: solution is based on single point positioning.

Default color to represent 'Fix' solution is green, 'Float' is yellow and 'Single' is red.

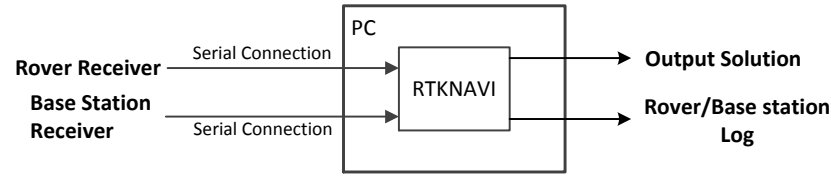


Figure 2.14. RTK GPS configuration through serial connection.

2.2.3. RTK GPS configuration

In RTK GPS positioning, base station is placed at fixed known/well-surveyed location, rover is moving or stationary based on requirement and there must be continuous transmission link between rover and base station for data transfer. Usually, rover and base station are at different places, which means that establishing data transmission link is a challenge. However, RTKLIB has built in AP, STRSVR, which can be used to resolve this issue. For example, to get base station measurement data at rover for calculating RTK GPS positioning, computer having base station receiver can configure STRSVR setting and send data to rover. There are different possible options explained below [3]:

1. First option; both base station and rover are connected to same Personal Computer (PC) through serial connection, as shown in Figure 2.14. This type of configuration is rarely possible except when both base station and point whose measurement is required are very close to each other. In this setup there is no need of STRSVR AP.
2. Second option; rover is connected to PC through serial connection while base station (consists of PC running STRSVR, and GPS receiver) is placed far away and is connected through WiFi TCP server and client setting of STRSVR and RTKNAVI respectively. Figure 2.15 shows this type of setup.
3. Third option; rover is connected through serial connection while base station is connected through mobile internet, as shown in Figure 2.16.
4. Fourth option; rover is connected through serial connection while base station is connected through NTRIP caster on internet, as shown in Figure 2.17.

Second option, shown in Figure 2.18, with slight modification is used in this thesis. Rover, which consists of Yuan10 receiver and GPS ANN-MS u-blox active antenna, is connected to PC, running RTKNAVI, through serial connection. Base station is placed at some distance from rover on known coordinate location. Base station consists of PC, running STRSVR, and Yuan10 receiver with GPS ANN-MS u-blox active antenna. WiFi router is placed in between rover and base station PCs and both PCs are connected to the router. Using base station PC as server and rover PC as client, STRSVR TCP server and RTKNAVI TCP client are configured accordingly.

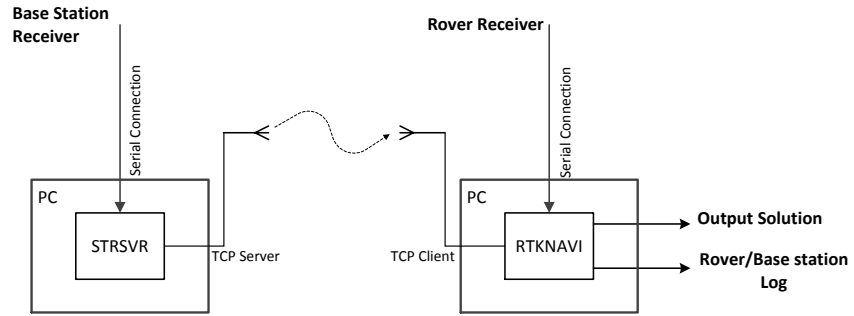


Figure 2.15. RTK GPS configuration through WiFi.

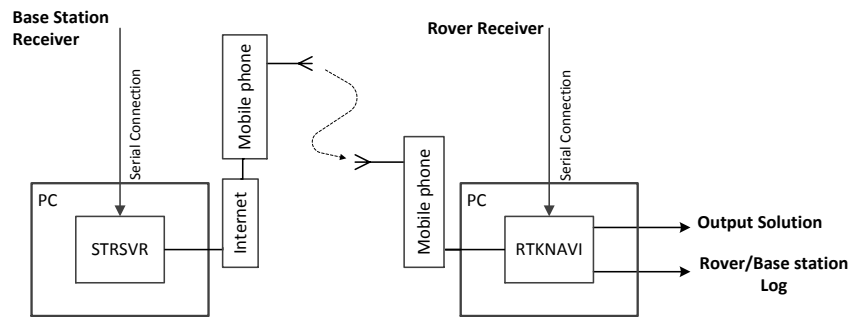


Figure 2.16. RTK GPS configuration through internet.

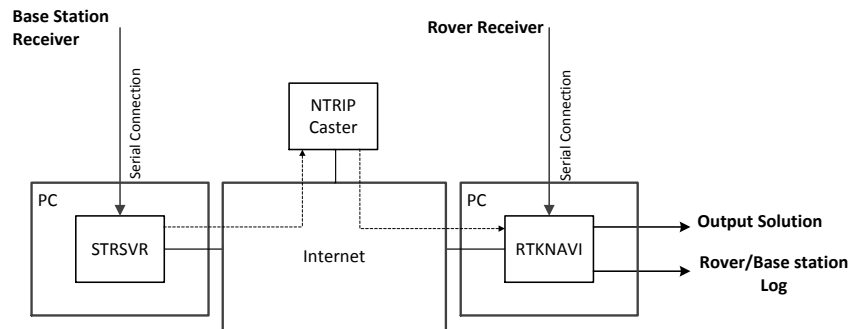


Figure 2.17. RTK GPS configuration through NTRIP Caster.

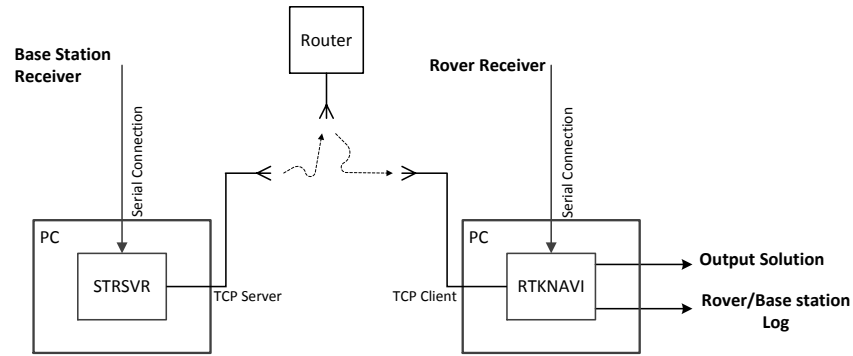


Figure 2.18. RTK GPS configuration used in thesis.

2.2.4. Testing and result

The testing of RTK GPS positioning is performed to check that system is working. Base station is placed at known position coordinate near Tampere University of Technology parking area (details are presented in next chapter section 3.1, here only results are presented to explain nature of positioning solution obtained from RTK GPS). Rover is also placed near to base station and both are connected to the same PC through serial connection (like first option explained in previous section of this chapter). Figure 2.19 shows E/N/U components of receiver position. Update rate of receiver is 1Hz and position at stationary point is collected for two minutes. Green dot represents 'Fix' solution while yellow represents 'Float' solution, moreover there are missing measurement points where solution is not available (cycle slips). Measurement was taken for approximately 2 minutes out of which measurement is missing for 9 seconds.

2.3. The Kalman filter for data fusion

Rudolf Emil Kalman published his paper on recursive predictive filter (known as Kalman filter) in 1960 which revolution the estimation field. This is same time when digital computer was introduced in market which made possible to implement Kalman filter in many real time applications. Kalman filter feature to estimate past, present and even future states is the main reason for its presence in many applications and current research. Kalman filter is applicable for both discrete and continuous time systems, however only discrete Kalman filter is discussed here. [24], [25], [26]

Kalman filter consists of two steps:

- First is 'Prediction' in which state is predicted with the help of dynamic model.
- Second is 'Correction' in which predicted state is corrected with the help of measurement model, such that error covariance is minimized.

Kalman filter is recursive in nature which means that above two steps repeat for each time step as shown in Figure 2.20. [24], [25]

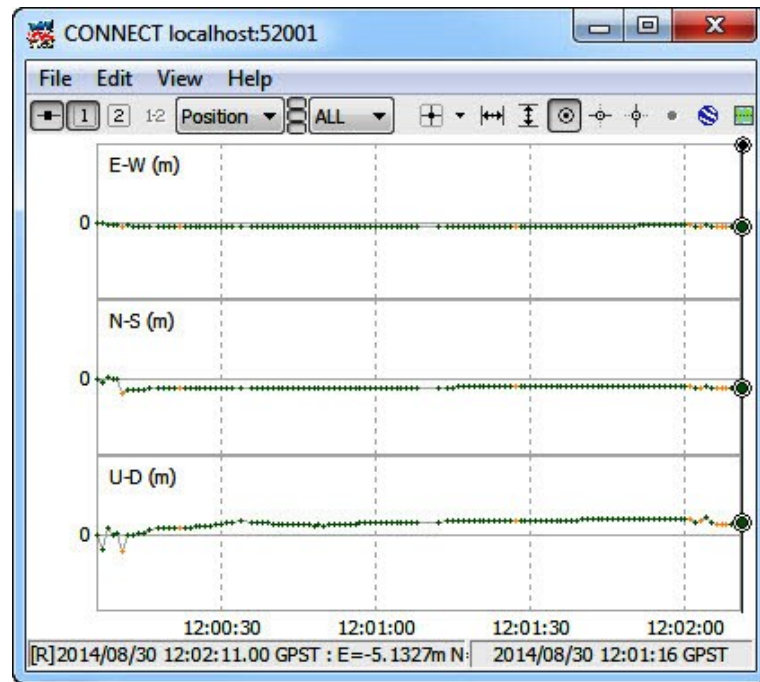


Figure 2.19. Sample testing result of RTK GPS positioning.

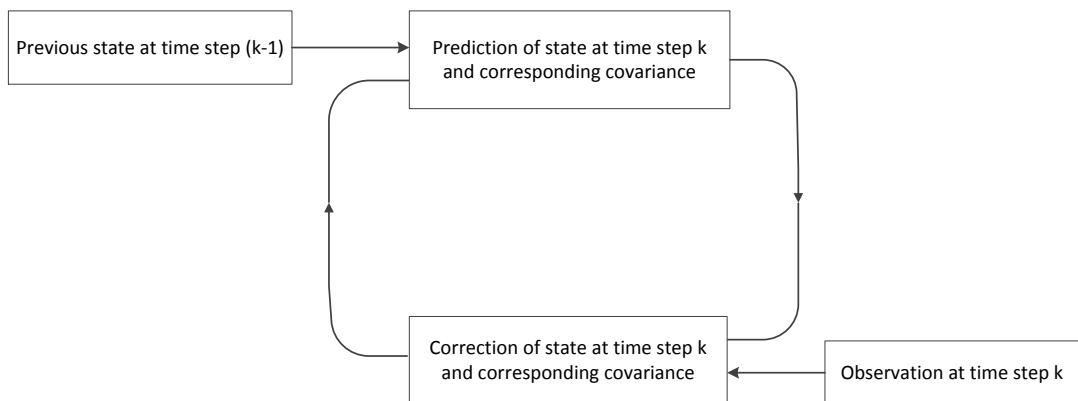


Figure 2.20. Kalman filter recursive steps.

Kalman filter has three basic components including state vector, dynamic model and measurement model which are explained below.

State vector x_k consists of elements representing variable of our interest. These variables, for example position, velocity, acceleration etc, cannot be measured directly rather they can be calculated indirectly from measurable variables. State vector x_k has two values at the same time i.e; a priori $x_k(-)$ and a posteriori $x_k(+)$. A priori $x_k(-)$ value is predicted value before update process while a posteriori $x_k(+)$ value after update process. [24], [25]

State vector transformation over time is described by dynamic model as following

$$x_k = F_{k-1}x_{k-1} + w_{k-1} \quad (2.7)$$

where

$$w_{k-1} \sim N(0, Q_{k-1}) \quad (2.8)$$

F_{k-1} is dynamic matrix, w_{k-1} is dynamic noise and Q_{k-1} is noise covariance matrix or system noise matrix. Moreover relation between state vector and measurement is given by measurement model as following

$$z_k = H_k x_k + v_k \quad (2.9)$$

where

$$v_k \sim N(0, R_k) \quad (2.10)$$

H_k is observation matrix, v_k is measurement noise matrix and R_k is noise covariance matrix or measurement noise matrix. [24], [25], [26]

Discrete kalman filter has following computational steps:

Step 1: Compute error covariance $P_k(-)$ and state vector $\hat{x}_k(-)$ using

$$P_k(-) = F_{k-1}P_{k-1}(+)F_{k-1}^T + Q_{k-1} \quad (2.11)$$

$$\hat{x}_k(-) = F_{k-1}\hat{x}_{k-1}(+) \quad (2.12)$$

Step 2: Compute Kalman gain K_k using

$$K_k = P_k(-)H_k^T [H_k P_k(-)H_k^T + R_k]^{-1} \quad (2.13)$$

Step 3: Compute updated error covariance $P_k(+)$ using

$$P_k(+) = [I - K_k H_k] P_k(-) \quad (2.14)$$

Step 4: Estimate the observational updated state $x_k(+)$ using

$$\hat{x}_k(+) = \hat{x}_k(-) + K_k[z_k - H_k\hat{x}_k(-)] \quad (2.15)$$

where z_k is input measurement. Moreover initial conditions \hat{x}_0 and P_0 are also assumed to be known [25].

Table 2.5 shows summary of discrete Kalman filter equations.

Table 2.5. Discrete Kalman filter equations summary.

Dynamic model: $x_k = F_{k-1} x_{k-1} + w_{k-1}$, $w_{k-1} \sim N(0, Q_{k-1})$
Measurement Model: $z_k = H_k x_k + v_k$, $v_k \sim N(0, R_k)$
Initial conditions: \hat{x}_0 and P_0
State estimate: $\hat{x}_k(-) = F_{k-1} \hat{x}_{k-1}(+)$
Error covariance: $P_k(-) = F_{k-1} P_{k-1}(+) F_{k-1}^T + Q_{k-1}$
State estimation observational update: $\hat{x}_k(+) = \hat{x}_k(-) + K_k [z_k - H_k \hat{x}_k(-)]$
Error covariance update: $P_k(+) = [I - K_k H_k] P_k(-)$
Kalman gain: $K_k = P_k(-) H_k^T [H_k P_k(-) H_k^T + R_k]^{-1}$

2.4. Summary

This chapter described theoretical background of UWB, RTK GPS and Kalman filter. BeSpoon phone equipped with pulse based UWB is used in thesis which uses two-way time-of-flight method for range calculation. In testing results it was found that tags have constant bias and have approximately same standard deviation.

Yuan10 carrier phase receiver with ANN-MS u-blox active antenna is used as RTK GPS receiver for both base station and rover. The transmission link between base station and rover is established through WiFi. It has been observed that solution is 'Fix' most of the time but have 'Float' solution as well as cycle slips problem.

The Kalman filter is recursive filter that can estimate past, present and future states as well. There are two main steps in Kalman filter, first is prediction of state and second correction of predicted state. Based on established theoretical background in this chapter, the next chapter explains methods and materials used in thesis.

3. UWB AND RTK GPS FUSION

RTK GPS positioning has high accuracy, positioning solution is for outdoor applications only, has high dynamic outdoor range but suffers from cycle slips problem and also requires good satellite visibility. UWB, on the other hand, can give highly accurate positioning solution but has low dynamic range. UWB can be used for both indoor and outdoor applications. Moreover, high bandwidth of UWB makes it multipath resistant and as result can be used in shadow areas. [27], [2]

Fusion of both RTK GPS and UWB positioning compensates the limitations of both and result in better performance system, as shown in Figure 3.1.

In this chapter, fusing configuration for UWB and RTK GPS positioning is presented first. After this, the Kalman filter parameters are explained in details. At the end, the method used for testing is elaborated.

3.1. UWB and RTK GPS fusion configuration

The fusion of UWB and RTK GPS requires having data from both simultaneously for computation. UWB data gives range and need to convert first into position and is coming from Android based operating system while RTK GPS data is coming through RTKLIB open source tool installed on Windows operating system. It is challenging to make available both data simultaneously on PC for fusion. Yuan10 receiver can give variable output data up to 20Hz rate but here 1Hz update rate is used for RTK GPS, moreover UWB has fixed 4Hz update rate. Both UWB and RTK GPS have different update rates and loosely coupled approach is used for fusion of both.

The configuration for RTK GPS positioning, explained in section 2.2.3, is used for overall fusion configuration with some modifications. This configuration is explained below and it is shown in Figure 3.2.

- PC1 which is connected to rover, PC2 which is connected to base station and BeSpoon phone equipped with UWB are connected to the same router.
- The base station data is transferred from PC2 to PC1 through router as explained previously and position is calculated with rover data at RTKNAVI running in PC1.
- The UWB data is transferred to PC1 through router with BeSpoon phone as server and PC1 as client. Android application package (APK) is built and installed on BeSpoon phone to transmit UWB data from BeSpoon phone to router through WiFi. To receive UWB data at PC1, java code is running at PC1 which is specifically written for this application.

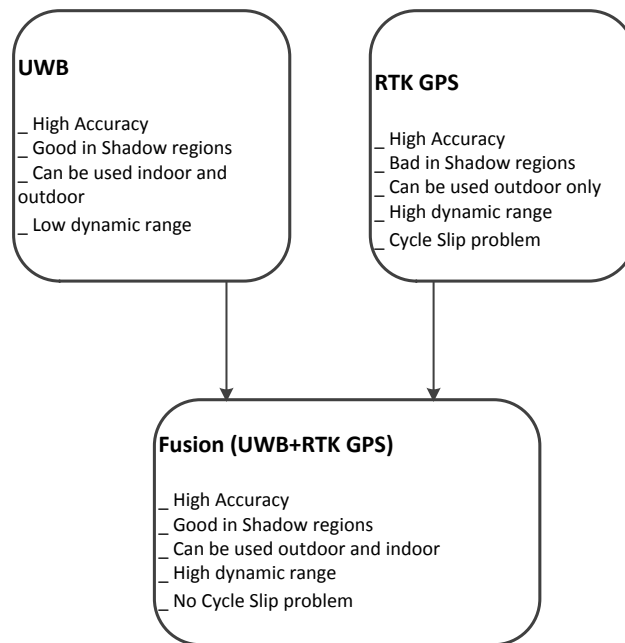


Figure 3.1. UWB and RTK GPS fusion properties.

- Now the PC1 has both RTK GPS positioning data and UWB data with time stamp which can be processed for fusion.

The data received from BeSpoon phone consists of tag number, distance in meter of tag from BeSpoon phone and system date and time (which helps in data processing). A sample data received from BeSpoon phone is shown in Figure 3.3.

Now we have two types of data; first UWB ranges from tags which are given in meter and relative to BeSpoon phone, and second the RTK GPS positioning coordinates in geodetic coordinate form (latitude and longitude). The following steps involves in fusion of both:

- Step 1: Convert UWB ranges to position in local coordinate system.
- Step 2: Convert RTK GPS positioning coordinate into local coordinate system.
- Step 3: Use Kalman filter for fusion of both positioning data.

Figure 3.4 shows process flow for fusion of UWB and RTK GPS data. Position from UWB range measurement is computed using trilateration [28]. Conversion from geodetic to local coordinate systems is done through a rotation matrix [2]. Here east and north directions are not exactly x and y coordinates of local coordinate system respectively which requires further rotation of coordinate frame to align them according to x and y coordinates of local coordinate system.

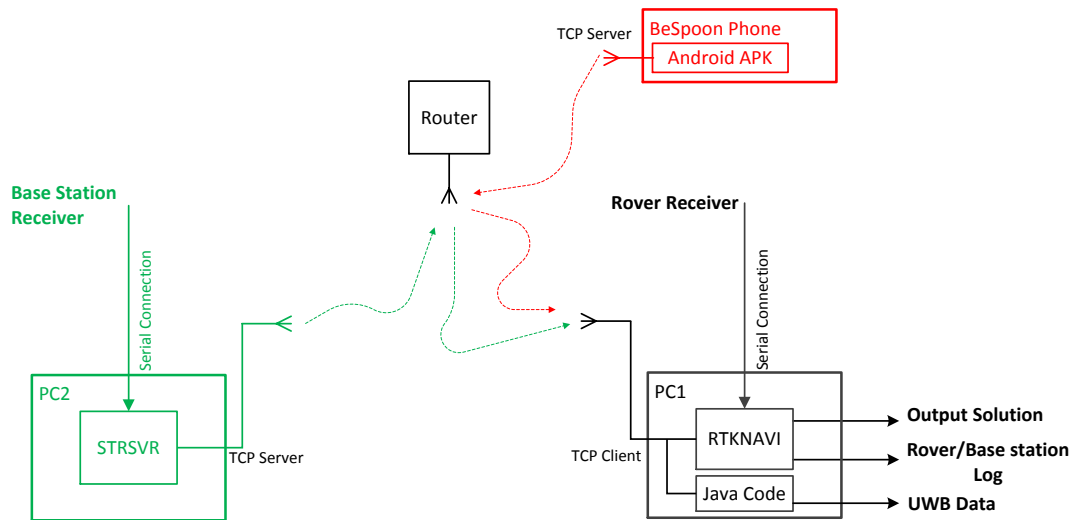


Figure 3.2. UWB and RTK GPS fusion configuration in our measurements.

File	Edit	Format	View	Help
systemTime = 2014/09/07 12:56:47.953,tag=one, Distance = 18.400848				
systemTime = 2014/09/07 12:56:47.973,tag=two, Distance = 13.708774				
systemTime = 2014/09/07 12:56:47.989,tag=three, Distance = 4.2449594				
systemTime = 2014/09/07 12:56:48.006,tag=four, Distance = 12.856488				
systemTime = 2014/09/07 12:56:48.017,tag=six, Distance = 6.9513946				
systemTime = 2014/09/07 12:56:48.087,tag=five, Distance = 14.097125				
systemTime = 2014/09/07 12:56:48.207,tag=one, Distance = 18.400848				
systemTime = 2014/09/07 12:56:48.223,tag=two, Distance = 13.708774				
systemTime = 2014/09/07 12:56:48.238,tag=three, Distance = 4.2449594				
systemTime = 2014/09/07 12:56:48.253,tag=four, Distance = 12.856488				
systemTime = 2014/09/07 12:56:48.270,tag=six, Distance = 6.9513946				
systemTime = 2014/09/07 12:56:48.338,tag=five, Distance = 14.097125				
systemTime = 2014/09/07 12:56:48.460,tag=one, Distance = 18.400848				
systemTime = 2014/09/07 12:56:48.472,tag=two, Distance = 13.708774				
systemTime = 2014/09/07 12:56:48.487,tag=three, Distance = 4.2449594				
systemTime = 2014/09/07 12:56:48.504,tag=four, Distance = 12.856488				
systemTime = 2014/09/07 12:56:48.518,tag=six, Distance = 6.9513946				
systemTime = 2014/09/07 12:56:48.588,tag=five, Distance = 14.097125				
systemTime = 2014/09/07 12:56:48.706,tag=one, Distance = 18.400848				
systemTime = 2014/09/07 12:56:48.727,tag=two, Distance = 13.708774				
systemTime = 2014/09/07 12:56:48.736,tag=three, Distance = 4.2449594				
systemTime = 2014/09/07 12:56:48.750,tag=four, Distance = 12.856488				
systemTime = 2014/09/07 12:56:48.766,tag=six, Distance = 6.9513946				
systemTime = 2014/09/07 12:56:48.841,tag=five, Distance = 14.097125				
systemTime = 2014/09/07 12:56:48.958,tag=one, Distance = 18.400848				
systemTime = 2014/09/07 12:56:48.973,tag=two, Distance = 13.708774				
systemTime = 2014/09/07 12:56:48.991,tag=three, Distance = 4.2449594				
systemTime = 2014/09/07 12:56:49.006,tag=four, Distance = 12.856488				
systemTime = 2014/09/07 12:56:49.021,tag=six, Distance = 6.9513946				
systemTime = 2014/09/07 12:56:49.086,tag=five, Distance = 14.097125				

Figure 3.3. Sample UWB data of approximately 1sec from BeSpoon phone.

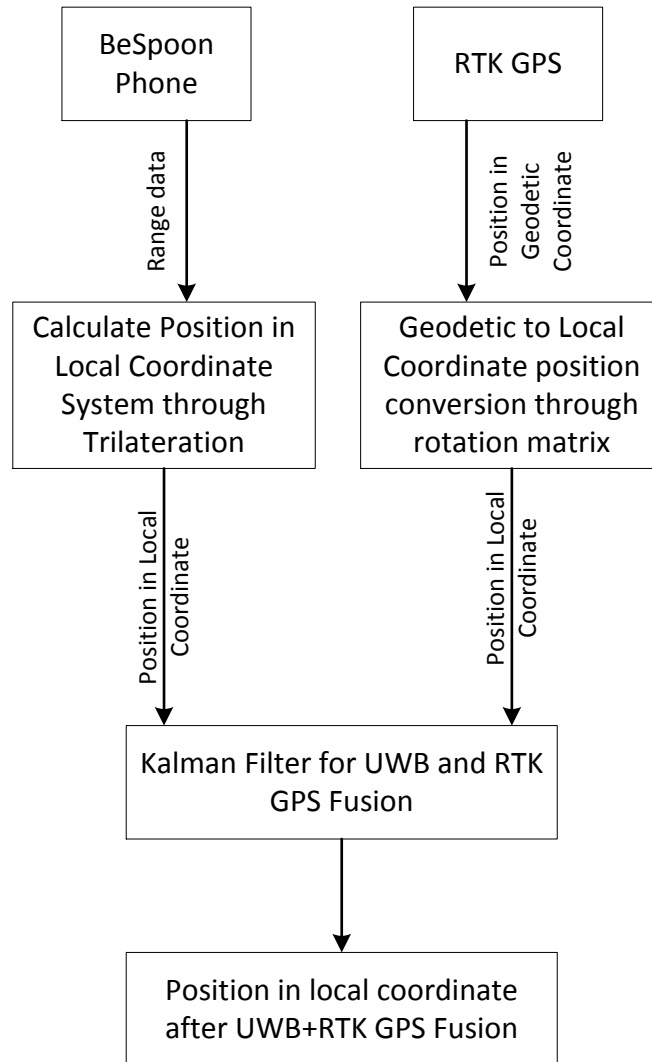


Figure 3.4. RTK GPS + UWB fusion process flow.

3.2. Kalman filter fusion parameters

As described previously, there are three components of Kalman filter, state vector, dynamic model and measurement model. Dynamic model has fundamental importance in navigation applications. There are two types of dynamic models; first type in which unknown parameter is considered as noise while other type incorporates known input. Motion of object can be in one, two or three dimensions but in this thesis motion in two dimensions is considered.

A constant velocity model is used as dynamic model and state and dynamic equation is given by [29]

$$x_k = \begin{bmatrix} x \\ y \\ v_x \\ v_y \end{bmatrix} \quad (3.1)$$

$$x_{k+1} = \begin{bmatrix} I_n & T I_n \\ 0_n & I_n \end{bmatrix} + \begin{bmatrix} \frac{T^2 I_n}{2} \\ T I_n \end{bmatrix} w_k \quad (3.2)$$

where $n=2 \times 2$, T is measurement sampling interval and w_k is process noise. x and y are position coordinates while v_x and v_y are velocity components of those coordinates. I_n is identity matrix of $n \times n$ and 0_n is zero matrix of $n \times n$. Q matrix will be

$$Q = GG^T \sigma^2 \quad (3.3)$$

where

$$G = \begin{bmatrix} \frac{T^2 I_n}{2} \\ T I_n \end{bmatrix} \quad (3.4)$$

σ is standard deviation which is considered to be equal to 10cm for both RTK GPS and UWB measurements. Moreover, after number of simulations, it has been observed that the result is optimum when Q has zero elements except diagonal.

Kalman filter is taking measurement directly from UWB and RTK GPS positioning solutions which means that measurement matrix is simple and given by

$$H = \begin{bmatrix} 1 & 0 & 0 & 0 \\ 0 & 1 & 0 & 0 \\ 1 & 0 & 0 & 0 \\ 0 & 1 & 0 & 0 \end{bmatrix} \quad (3.5)$$

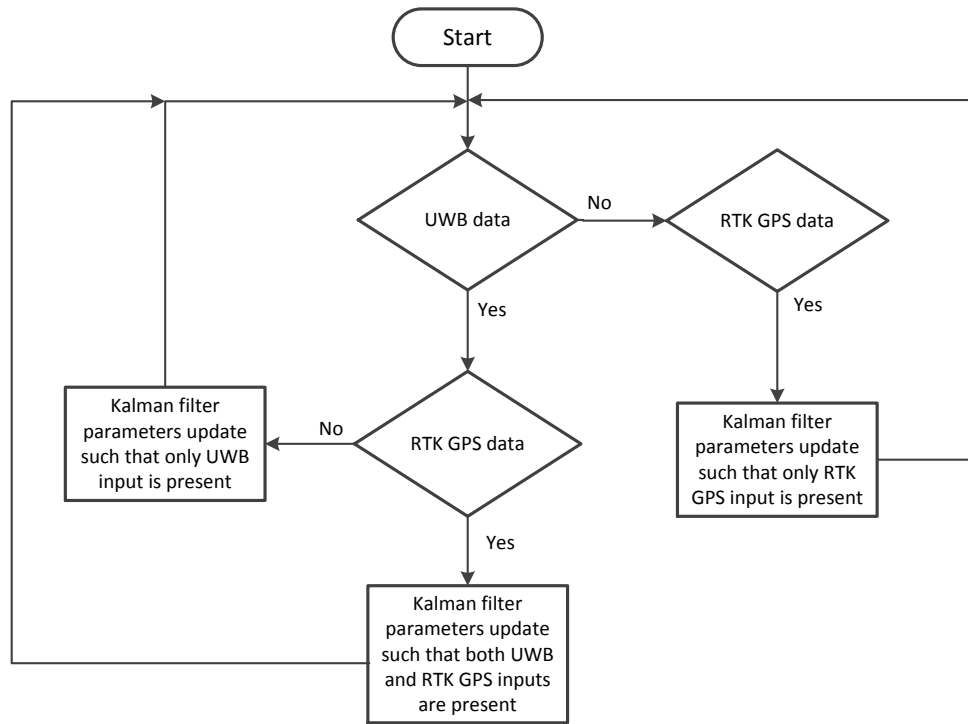


Figure 3.5. Fusion filter algorithm.

while R matrix is given by [21]

$$R = \begin{bmatrix} \sigma & 0 & 0 & 0 \\ 0 & \sigma & 0 & 0 \\ 0 & 0 & \sigma & 0 \\ 0 & 0 & 0 & \sigma \end{bmatrix} \quad (3.6)$$

The initial position x_0 is given as starting point of measurement while P_0 is given as

$$P_0 = \sigma \begin{bmatrix} 1 & 0 & 0 & 0 \\ 0 & 1 & 0 & 0 \\ 0 & 0 & 1 & 0 \\ 0 & 0 & 0 & 1 \end{bmatrix} \quad (3.7)$$

UWB and RTK GPS have different update rates. This means that the filter should be able to work in three different situations. First, when both UWB and RTK GPS data is present, second, when only UWB data is present and third, when only RTK GPS data is present. Figure 3.5 shows the algorithm of the filter. After setting all Kalman filter parameters, state of system is predicted and corrected according to steps explained in section 2.3 of chapter 02.



Figure 3.6. Photo of a known coordinate point.

3.3. Testing method

The top floor of Tampere University of Technology (TUT) parking building is selected for testing. One corner of parking area has known coordinates in ETRS-GK24 format (detail of surveyed points is at [30]). This point is used as fixed known coordinate point for base station of RTK GPS positioning. The conversion of ETRS-GK24 to WGS84 coordinate system is done through National Land Survey of Finland website. The coordinate detail of surveyed point is presented in Table 3.1. Figure 3.6 is a photo of a known coordinate point.

Table 3.1. Coordinate detail of surveyed point.

Coordinates in ETRS89-GK24FIN form:

Latitude = 6815501.704

Longitude = 24492311.032

Height = 145.435

Converted to WGS84 coordinate system:

Latitude = 61.448694910

Longitude = 23.855854700

Height = 145.435

Figure 3.7 shows the Google Earth aerial view of testing setup. A base station consisting of PC2, Yuan10 receiver and L1 antenna is placed at corner of TUT parking area near point with known coordinates. The testing area is on other corner of TUT parking. The

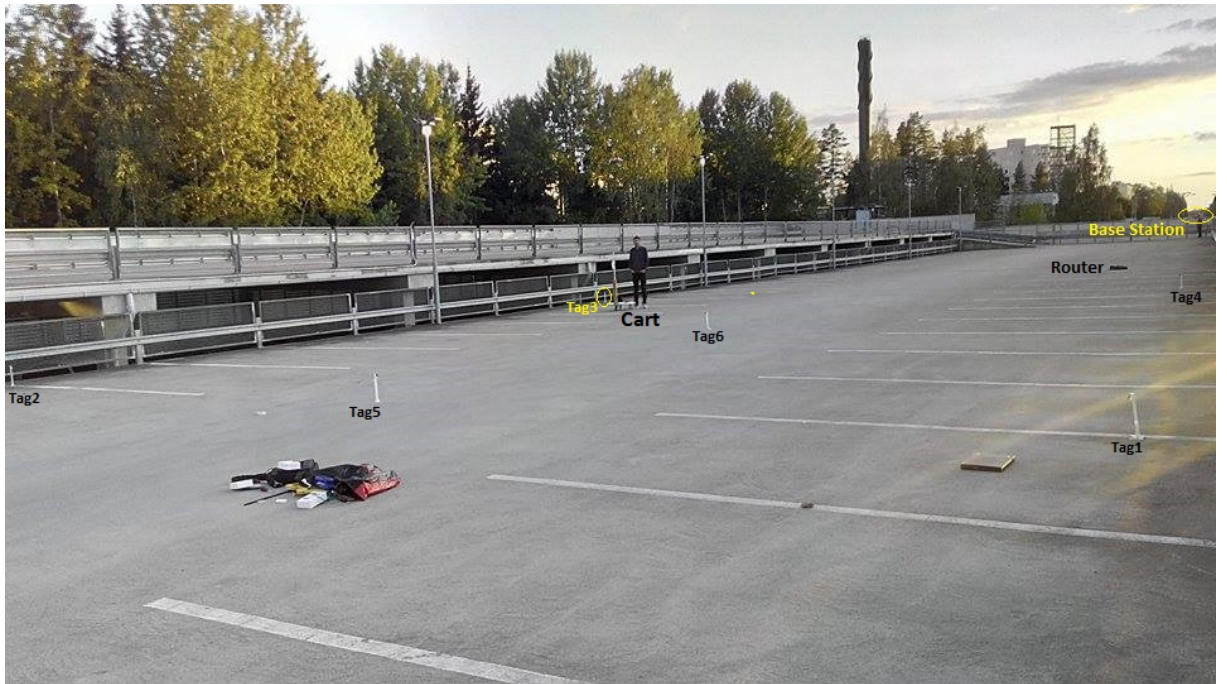


Figure 3.8. Front view of testing setup.

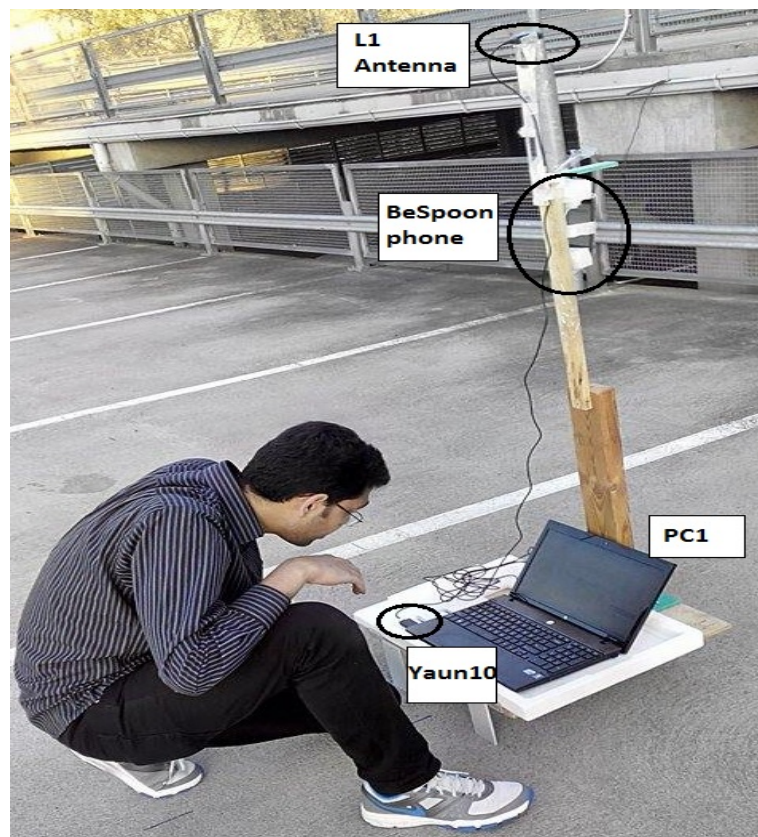


Figure 3.9. Cart.

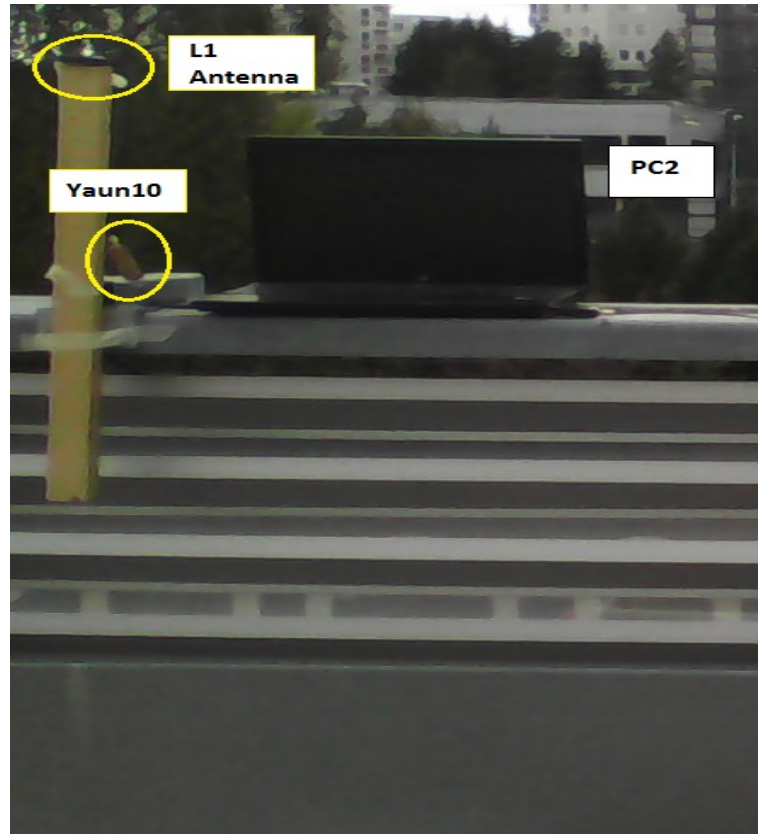


Figure 3.10. Base station.

3.4. Summary

This section describes a computational and experimental framework for fusion of UWB and RTK GPS. For RTK GPS positioning solution, base station and rover are connected through WiFi. BeSpoon phone UWB data is transferred to PC1 through WiFi as well. BeSpoon phone UWB data consists of range and tag relative to BeSpoon phone while RTK GPS positioning solution consists of geodetic coordinate (latitude and longitude). Trilateration method is used to calculate position through UWB ranges in local coordinate system. RTK GPS positioning solution is also converted to local coordinate system through rotation matrix.

A constant velocity model is used as dynamic model in Kalman filter. TUT parking area is selected for testing. A corner point with known coordinate is used for base station while tags placement and track to follow is drawn through Leica TPS1200. After configuring, measurements are taken and results are presented in next chapter.

4. RESULTS AND DISCUSSION

After the measurement setup at TUT parking area, the measurements are done. Measurement data is post processed and results are presented in this chapter. Measurement setup shows six UWB tags while in post process results are also checked with four tags. During the measurement no cycle slip occurred because measurement is done in small area of $100\text{m} \times 30\text{m}$ and satellite visibility was good. To check the behavior of the filter cycle slip is simulated.

In this chapter, results of measurement with six UWB tags are presented. After this, results with four UWB tags are presented. At the end of chapter comparison of RTK GPS, UWB, and fusion of both results are presented in term of root-mean-square (RMS) error.

4.1. Result with 6 UWB tags

Measurement setup is same as explained in last chapter. All six tags are used in UWB positioning solution. After receiving positioning data from RTK GPS and range data from UWB, fusion filter process both data and overall position is calculated from fusion of UWB and RTK GPS. Figure 4.1 shows the obtained results. Dark black dashed line shows reference track to be followed. Blue dot points shows RTK GPS positioning solution, green continuous line shows UWB positioning solution and continuous red line shows fusion of both UWB and RTK GPS positioning solutions. Tag positions are shown in magenta stars. Starting point is highlighted with black arrow and measurement consists of one complete loop of reference track.

To analyze the result in a better way, measurement track can be divided into three sub tracks, as shown in Figure 4.2. Table 4.1 shows root-mean-square (RMS) error for three sub tracks. In sub track 1, overall fusion solution has better accuracy compared to RTK GPS solution because of input from UWB. Which indicates that filter can overcome jumps in RTK GPS positioning solution as well. In sub track 2, when RTK GPS and UWB have good solution accuracy, resultant fusion filter solution has very good accuracy. In sub track 3, when RTK GPS and UWB both solutions have very good accuracy, resultant fusion solution have even better accuracy compared to individual one.

Figure 4.3 shows fusion filter result with cycle slip. Cycle slip is simulated by removing input from RTK GPS for three seconds. Moreover Table 4.2 shows comparison of root-mean-square (RMS) error with and without cycle slip for sub track 2. Result indicates that filter is behaving as expected, when input from RTK GPS is missing (cycle slip) then input from UWB keep filter on track.

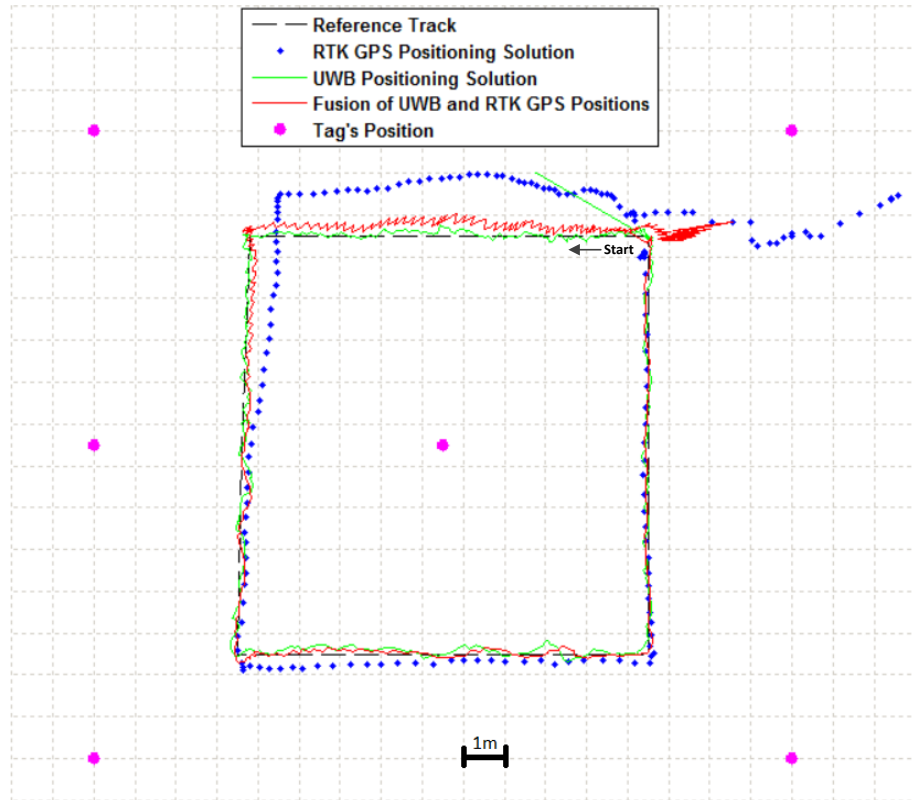


Figure 4.1. Result with six UWB tags.

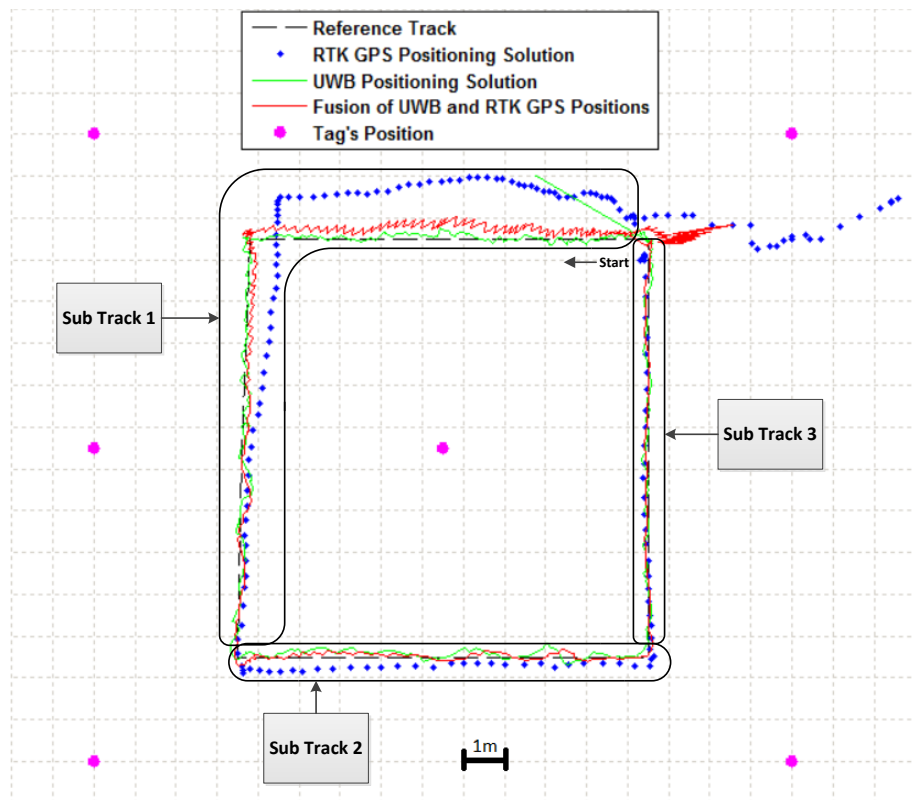


Figure 4.2. Track is divided into three sub tracks.

Table 4.1. RMS error (m) comparison of RTK GPS, UWB and fusion of UWB and RTK GPS results.

Track	RTK GPS	UWB	UWB+RTK GPS Fusion	Percentage improvement compared to RTK GPS
Sub Track 1	0.910	0.133	0.304	66%
Sub Track 2	0.234	0.122	0.070	70%
Sub Track 3	0.065	0.063	0.053	18%

Table 4.2. RMS error (m) comparison of fusion results with and without cycle slip of sub track 2

Track	UWB+RTK GPS Fusion
Without Cycle Slip	0.070
With Cycle Slip	0.071

4.2. Result with 4 UWB tags

In previous section, all six tags were used for UWB positioning solution. This section describes the effect of tags position and their number in UWB positioning solution as well as effect on overall fusion solution. Three different types of tag's placement scenarios have been investigated here. First placement consists of tag1, tag2, tag3 and tag4. Second placement consists of tag1, tag4, tag5 and tag6. Third placement consists of tag1, tag3, tag4 and tag6. After calculation, it has been observed that considering tag1, tag2, tag3 and tag4 gives same result as in case of six tags.

Figure 4.4 shows result for second scenario and Figure 4.5 shows result for third scenario. Table 4.3 shows comparison of all three scenarios in term of root-mean-square (RMS) error for three sub tracks similar to previous section.

Table 4.3. RMS error (m) comparison of RTK GPS, UWB and fusion of UWB and RTK GPS results with 4 tags

Track	First scenario			Second scenario			Third scenario		
	RTK GPS	UWB	Fusion	RTK GPS	UWB	Fusion	RTK GPS	UWB	Fusion
Sub track 1	0.910	0.133	0.304	0.910	0.194	0.354	0.910	0.224	0.296
Sub track 2	0.234	0.122	0.070	0.234	0.130	0.126	0.234	0.140	0.069
Sub track 3	0.065	0.063	0.053	0.065	0.070	0.058	0.065	0.096	0.076

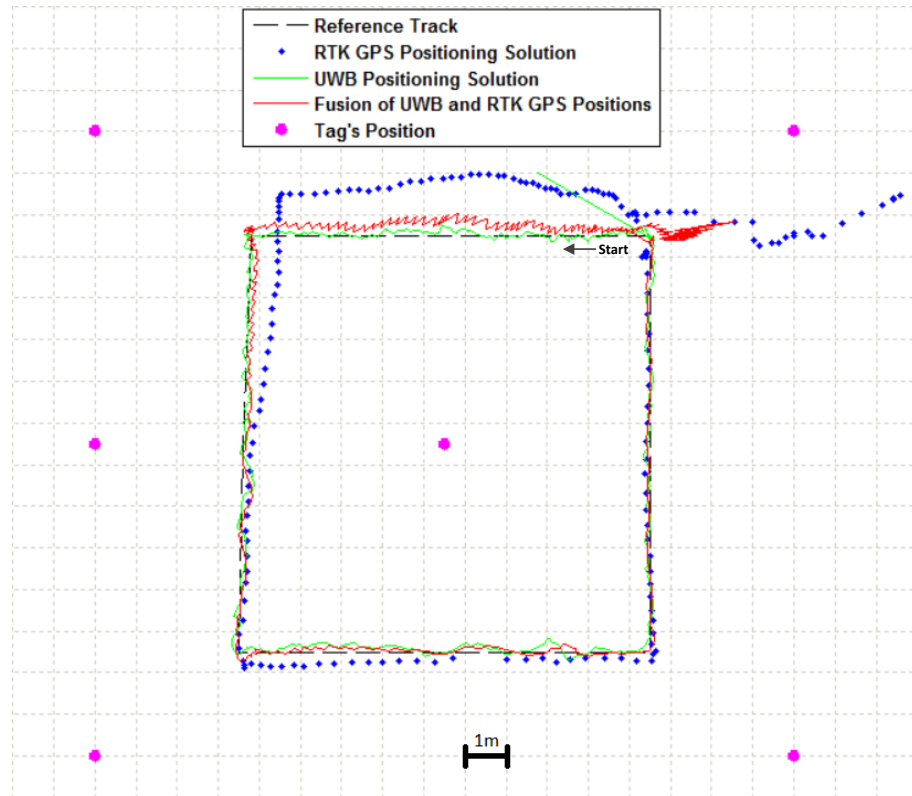


Figure 4.3. Result with cycle slip (simulated).

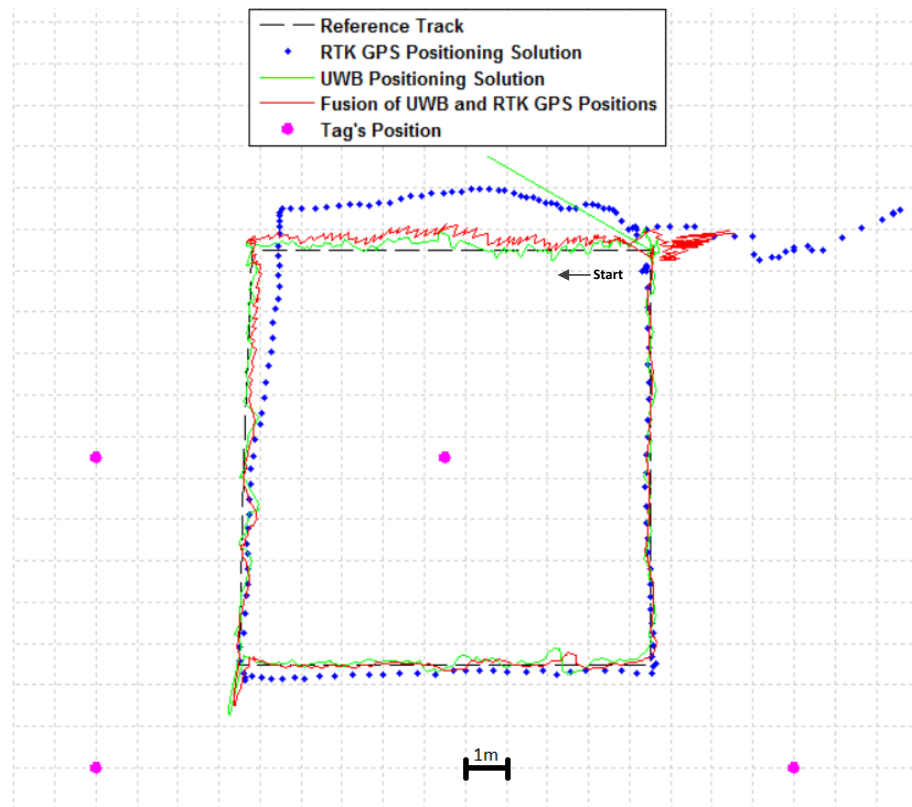


Figure 4.4. Result with four UWB tags second scenario.

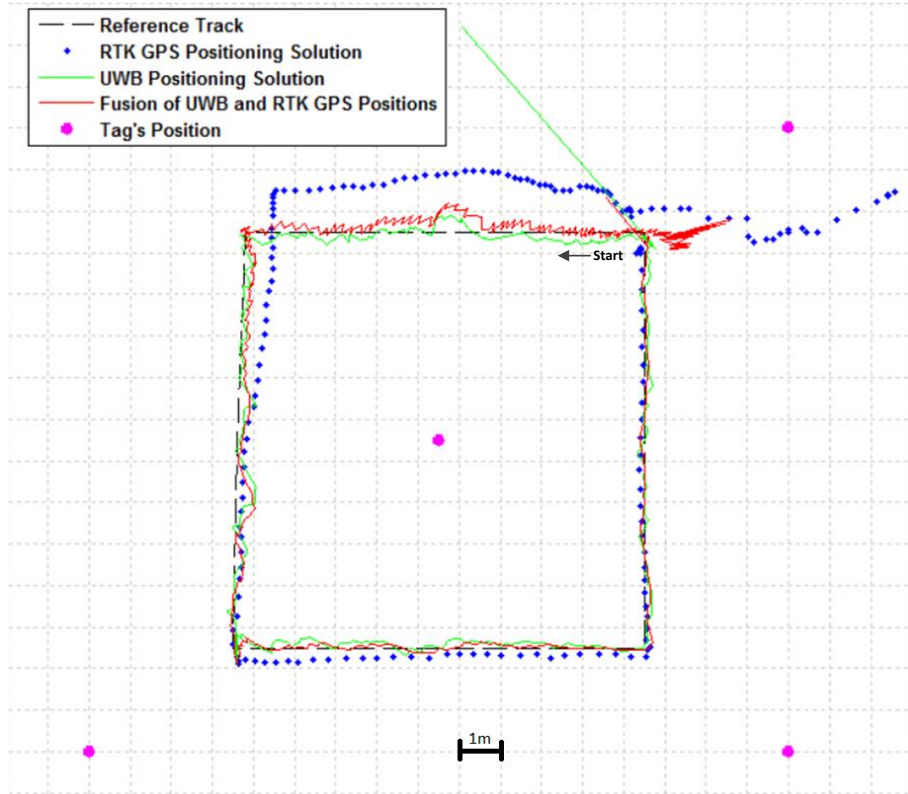


Figure 4.5. Result with four UWB tags third scenario.

4.3. Comparison of results

This section presents overall result comparison with some discussion on results. Table 4.4 shows overall results with 6 and 4 UWB tags for three sub tracks.

UWB uses trilateration for position calculation; it means placement of tags will have considerable impact on overall positioning result. Tag's placement geometry should be favorable to position calculated from their distances to avoid singularities and low precision. Tags must not place on straight line to avoid singularities. Based on these facts, we present below the detailed analysis of obtained results.

Results of first scenario with 4 tags and results with 6 tags are exactly same, indicating that two extra tags don't improve positioning solution further. Moreover it can be seen that best possible option is first scenario with 4 tags in term of placement and numbers of tags in measurements but on the other hand in estimation, it is always better to have data from as many sensors as possible.

Results of second scenario with 4 tags highlight two important points. First, the sub track 2 and sub track 3 have approximately the same UWB and fusion of UWB and RTK GPS RMS errors compared to first scenario with 4 tags and with 6 tags, which is due to fact that both tracks are mostly in between the region of tag's placement. Second, the sub track 1 gives more RMS error compared to the first scenario with 4 tags and with 6 tags which is due the fact that mostly sub track 1 is outside of region in between the tag's placement.

Although UWB results in the third scenario with 4 tags have high RMS error for all sub

Table 4.4. *RMS error (m) comparison of RTK GPS, UWB and fusion of UWB and RTK GPS results with 4 and 6 tags*

Track	6 Tags			4 Tags								
	RTK GPS	UWB	Fusion	First scenario			Second scenario			Third scenario		
				RTK GPS	UWB	Fusion	RTK GPS	UWB	Fusion	RTK GPS	UWB	Fusion
Sub track 1	0.910	0.133	0.304	0.910	0.133	0.304	0.910	0.194	0.354	0.910	0.224	0.296
Sub track 2	0.234	0.122	0.070	0.234	0.122	0.070	0.234	0.130	0.126	0.234	0.140	0.069
Sub track 3	0.065	0.063	0.053	0.065	0.063	0.053	0.065	0.070	0.058	0.065	0.096	0.076

tracks yet fusion results of sub track 1 and sub track 2 have less RMS error as compared to other scenarios. The reason is as following: UWB and RTK GPS shows opposite deviation from the reference track and as a coincidence fusion of both gives better result, as can be seen from Figure 4.5. High RMS error for UWB positioning solution for third scenario is due to the reason that three (tag 1, tag3 and tag6) out of four tags are placed in straight line.

4.4. Summary

Results with 4 and 6 UWB tags have been presented. Comparison shows that best results can be obtained with first scenario with 4 tags in presented measurement scenarios. Moreover the placement and number of tags have considerable impact on overall fusion results. Tags should be placed such that movement area is in between those tags and also tags should not be placed on straight line. Next chapter presents thesis conclusion and future work that can be done related to this.

5. CONCLUSIONS AND FUTURE WORK

5.1. Conclusions

The goal of the thesis is to overcome the positioning blackouts due to the cycle slips in Real Time Kinematic (RTK) GPS by augmenting the GPS RTK with the UWB. UWB and RTK GPS had to be studied along with the Kalman filter for fusion of both. RTK GPS uses carrier phase measurement and suffers of cycle slips problem. Centimeter level accuracy can be achieved with RTK GPS positioning solution, but cycle slips problem need to overcome to maintain such accuracy. UWB with ranging property is good candidate for such application because it also gives centimeter level of range accuracy.

RTK GPS positioning solution requires three steps, placement of base station at known point, establishment of continuous transmission connection between rover and base station and calculation of position by rover through difference of measurements. RTKLIB which is open source software tool is used for RTK GPS positioning solution. This tool has different APs for different purposes. There can be different possible configurations for RTK GPS positioning and Figure 2.18 shows the used configuration in the thesis. Yuan10 receiver consists of Skytraq S1315F-RAW chip and u-blox active antenna are used as base station and rover receivers.

UWB uses two-way time-of-flight method for ranging. The huge bandwidth in frequency domain corresponds to short pulses in time domain. The large frequency bandwidth of UWB makes it suitable for positioning and navigation application. Multipath resistance, high accuracy, low cost and low power implementation are other features of UWB. BeSpoon phone equipped with UWB has been used in the thesis. Figure 2.8 and Figure 2.9 shows static and dynamic testing results respectively of BeSpoon phone and its tags. Constant bias is present in UWB range for all tags which is catered in Kalman filter during fusion of UWB and RTK GPS.

Figure 3.2 shows the system setup configuration for measurement. UWB gives range and RTK GPS gives position in GPS (latitude and longitude) coordinate. Trilateration is used to calculate position in local coordinate through UWB range and rotation matrix is used to convert GPS coordinate to local coordinates. Figure 3.4 shows system process flow and Figure 3.7 shows Google Earth top view of system setup. Tampere University of Technology (TUT) parking building top floor is used for measurement.

The Table 4.4 shows overall results of the thesis. The results indicates that fusion of UWB and RTK GPS gives better results with and without cycle slip cases compared to individual RTK GPS. Moreover the number of tags and their placement have impact on

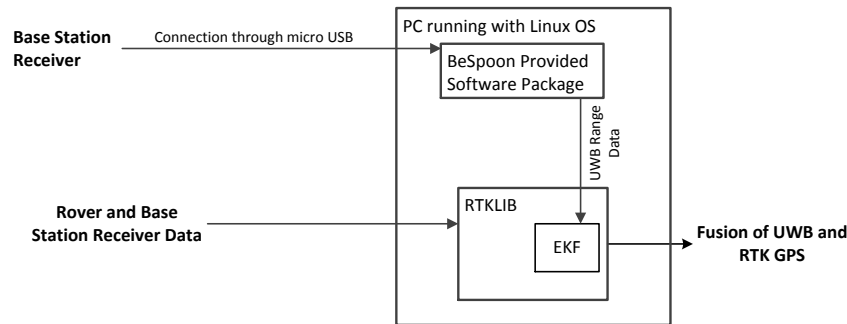


Figure 5.1. Proposed hexacopter navigation system configuration for future studies.

overall results as well. The best scenario is first with 4 tags usage (tag1, tag2, tag3 and tag4). Based on the obtained results it can be concluded that UWB augmentation to RTK GPS provided fruitful results. Moreover based on Table 4.4 results it can also be seen that UWB has centimeter level of positioning accuracy comparable to RTK GPS. This indicates that UWB can also be used as replacement of RTK GPS.

5.2. Future work

This thesis uses loosely coupled approach for fusion of UWB and RTK GPS. Tightly coupled approach can be tried as well with BeSpoon phone UWB and RTK GPS. In tightly coupled approach UWB range can be used directly instead of first position calculation through UWB range. This also make possible to use only one tag instead of four or six tags.

Moreover BeSpoon phone have some other sensors such as accelerometer etc. which can be used as well in fusion process. Although measurement from these is not of high accuracy because usually they are less accurate yet experiment can be made to check the behavior. It can also be possible to use external inertial navigation system (INS) with UWB and RTK GPS to further stabilize the overall fusion system.

The ASE department's hexacopter would be good application for thesis result. BeSpoon phone is small and light enough to be carried as payload on hexacopter. This can be used in two ways. The first method is the same as explained in the thesis but one would need to work in Linux OS and to extend the studies to three dimensions. Moreover overall fusion results need to be converted to GPS coordinate system with rotation matrix. The second approach is to feed UWB range measurements to Extended Kalman filter (EKF) of RTKLIB. RTKLIB is open source software which means changes to source code can be made easily. Reference [3] explains in detail about the EKF parameters of RTKLIB. In order to get UWB range measurements, BeSpoon provides software packages supported by Linux OS. Figure 5.1 shows a proposed hexacopter navigation system configuration for future studies.

REFERENCES

- [1] Z. Sahinoglu, S. Gezici and I. Guvenc, " Ultra-wideband positioning systems: theoretical limits, ranging algorithms, and protocols", Cambridge University Press, pp. 1-42, 2008.
- [2] P. Misra and P. Enge, "Global positioning system signals, measurements, and performance", Ganga-Jamuna Press, Lincoln, Massachusetts, 01773, 2006.
- [3] T. Takasu, RTKLIB ver. 2.4.2 Manual [Accessed 14.10.2014]. Available: http://www.rtklib.com/prog/manual_2.4.2.pdf.
- [4] E. D. Kaplan and C. J. Hegarty, "Understanding GPS: principles and applications", 2nd edition, Artech House, Inc., 2006.
- [5] A. Gorski and G. Gerten, "Do we need augmentation systems?", European Journal of Navigation, Volume 5, Number 4, September 2007.
- [6] G. D. MacGougan, " Real-Time Kinematic surveying using tightly-coupled GPS and ultra-wideband ranging", Doctor of Philosophy Thesis, The University of Calgary, August, 2009.
- [7] G. Opshaug and P. Enge, "Integrated GPS and UWB navigation system: motivates the necessity of non-interference", IEEE UWBST, pp. 123-127, 2002.
- [8] E. Broshears, "Ultra-wideband radio aided carrier phase ambiguity resolution in real-time kinematic GPS relative positioning", A thesis submitted to the Graduate Faculty of Auburn University, August 3, 2013.
- [9] BeSpoon Phone [Accessed 14.10.2014]. Available: <http://spoonphone.com/en/>.
- [10] T. Barrett, "History of ultra wideband communications and radar", Part I. UWB Communications, International Microwave Journal, 44(1), pages 22-56, 2001.
- [11] G. Ross, "Transmission and reception system for generating and receiving baseband duration pulse signals without distortion for short base-band pulse communication system", U.S. Patent 3728632, 1973.
- [12] FCC, "Revision of part 15 of the commissions rules regarding ultra-wideband transmission systems", First Report and Order in ET Docket No. 98-153, Adopted February 14, 2002, released July 15, 2002.
- [13] FCC, "Revision of part 15 of the commissions rules regarding ultra-wideband transmission systems", Second Report and Order and Second Memorandum Option and

Order in ET Docket No. 98-153, Adopted December 15, 2004, released December 16, 2004.

- [14] S. A. Zekavat and R. M. Buehrer, "Position location : theory, practice, and advances", IEEE series on digital mobile communication, ePDF ISBN: 9781118104774, pages 1-63, 2011.
- [15] S. Gezici, Z. Tian, G. B. Giannakis, H. Kobayashi, A. F. Molisch, H. V. Poor and Z. Sahinoglu, "Localization via ultra-wideband radios: a look at positioning aspects of future sensor networks", IEEE Signal Processing Magazine, July 2005.
- [16] IEEE802-15.4a, "Part 15.4: Wireless medium access control and physical layer specifications for low-rate wireless personal area networks", IEEE Standards, 2007.
- [17] Dart RTLS User Guide, Provided with equipment, A ZEBRA Technologies Company.
- [18] I. I. Immoreev and V. Fedotov, "Ultra wideband radar systems: advantages and disadvantages ", IEEE UWBST, 2002.
- [19] R. Piche, "Introduction to statistical data analysis for engineers and scientists", CreateSpace Independent Publishing Platform, pages 95-101, May 24, 2013.
- [20] Leica TPS1200, User Manual, Leica Geosystems [Accessed 14.10.2014]. Available: http://www.surveyequipment.com/PDFs/TPS1200_User_Manual.pdf.
- [21] Yuan10, OneTalent GNSS [Accessed 14.10.2014]. Available: <http://www.onetalent-gnss.com/ideas/usb-hw-receivers/yuan10>.
- [22] ANN-MS active GPS antenna, u-blox, Datasheet [Accessed 14.10.2014]. Available: [http://www.u-blox.com/images/downloads/Product_Docs/ANN_Data_Sheet\(GPS-X-02021\).pdf](http://www.u-blox.com/images/downloads/Product_Docs/ANN_Data_Sheet(GPS-X-02021).pdf).
- [23] RTKLIB: An open source program package for GNSS positioning [Accessed 14.10.2014]. Available: <http://www.rtklib.com/>.
- [24] R. Kleinbauer, "Kalman filtering implementation with Matlab", Study report in the field of study Geodesy and Geoinformatics at University Stuttgart, November 2004.
- [25] M. S. Grewal and A. P. Andrews, "Kalman filtering: theory and practice", Prentice Hall information and systems sciences series, ISBN 0-13-211335-X, pages 106-115, 1993.
- [26] R. G. Brown, "Introduction to random signal analysis and Kalman filtering", John Wiley Sons, Inc., ISBN 0-471-08732-7, pages 195-205, 1983.

- [27] J. B. Sillero, "Sensor fusion methods for indoor navigation using UWB radio aided INS/DR", Master's Degree Project, KTH Electrical Engineering Sweden, July 2012.
- [28] W. S. Murphy Jr. and W. Hereman, "Determination of a position in three dimensions using trilateration and approximate distances", November 28, 1999.
- [29] F. Gustafsson, "Statistical sensor fusion", Holmbergs i Malmö AB, Sweden, ISBN 978-91-44-05489-6, pages 337-340, 2010.
- [30] Surveyed points details website [Accessed 14.10.2014]. Available: <http://www.paikkatietoikkuna.fi/web/en/map-window>.